Biochem. J. (2014) **459**, 467–478 (Printed in Great Britain) doi:10.1042/BJ20130732

The cysteine desulfurase IscS of *Mycobacterium tuberculosis* is involved in iron–sulfur cluster biogenesis and oxidative stress defence

Jan RYBNIKER*†[1], Florence POJER*, Jan MARIENHAGEN‡, Gaëlle S. KOLLY*, Jeffrey M. CHEN*, Edeltraud VAN GUMPEL†, Pia HARTMANN†§ and Stewart T. COLE*

*Global Health Institute, Ecole Polytechnique Fédérale de Lausanne (EPFL), CH-1015 Lausanne, Switzerland
†1st Department of Internal Medicine, University of Cologne, D-50937 Cologne, Germany
‡Institut für Bio- und Geowissenschaften, IBG-1: Biotechnologie, Forschungszentrum Jülich GmbH, D-52425 Jülich, Germany
§Institute for Medical Microbiology, Immunology and Hygiene, University of Cologne, D-50937 Cologne, Germany

The complex multiprotein systems for the assembly of protein-bound iron–sulfur (Fe–S) clusters are well defined in Gram-negative model organisms. However, little is known about Fe–S cluster biogenesis in other bacterial species. The ISC (iron–sulfur cluster) operon of *Mycobacterium tuberculosis* lacks several genes known to be essential for the function of this system in other organisms. However, the cysteine desulfurase IscSMtb (Rv number Rv3025c; Mtb denotes *M. tuberculosis*) is conserved in this important pathogen. The present study demonstrates that deleting *iscS*Mtb renders the cells microaerophilic and hypersensitive to oxidative stress. Moreover, the Δ*iscS*Mtb mutant shows impaired Fe–S cluster-dependent enzyme activity, clearly indicating that IscSMtb is associated with Fe–S cluster assembly. An extensive interaction network of IscSMtb with Fe–S proteins was identified, suggesting a novel mechanism of sulfur transfer by direct interaction with apoproteins. Interestingly, the highly homologous IscS of *Escherichia coli* failed to complement the Δ*iscS*Mtb mutant and showed a less diverse protein-interaction profile. To identify a structural basis for these observations we determined the crystal structure of IscSMtb, which mirrors adaptations made in response to an ISC operon devoid of IscU-like Fe–S cluster scaffold proteins. We conclude that in *M. tuberculosis* IscS has been redesigned during evolution to compensate for the deletion of large parts of the ISC operon.

Key words: iron–sulfur cluster, IscS, IscU, protein–protein interaction, tuberculosis.

INTRODUCTION

Iron–sulfur (Fe–S) proteins and sulfur-containing cofactors are ubiquitous in all kingdoms of life and participate in a plethora of fundamental processes of biosynthetic pathways [1–4]. Fe–S proteins are involved in redox systems, central metabolism, respiration, gene regulation, RNA modification, and DNA repair and replication. In humans, insufficiency in Fe–S cluster biogenesis leads to some forms of sideroblastic anaemia as well as Friedreich's ataxia, a degenerative disease of the nervous system [1].

To understand the mechanism by which these fragile clusters are built, maintained and repaired has been of major interest to the research community over the past two decades [2,3]. Owing to the multitude of Fe–S proteins (>150 predicted proteins in *Escherichia coli*), their biosynthetic machineries have a major effect on most essential metabolic pathways. Knowledge of the individual differences in Fe–S cluster biogenesis of different bacterial species may provide tools to better understand evolutionary adaptations made in response to changing habitats and strategies to combat bacterial pathogens.

To date, our knowledge of bacterial Fe–S cluster assembly mechanisms is based primarily on investigations made in Gram-negative bacteria. *E. coli* uses two multiprotein systems, ISC (iron–sulfur cluster) and SUF (sulfur metabolism), to assemble and deliver Fe–S clusters. The SUF system is active only under conditions of oxidative stress or iron limitation, whereas the ISC system is believed to be the housekeeping system that serves most Fe–S proteins and enzymes using sulfur as their cofactor [5,6]. Both systems function as complex machineries in which up to eight individual proteins encoded by the *iscRSUA-hscBA-fdx* operon (Figure 1) or the *sufABCDSE* operon participate in a multistep process which delivers [2Fe–2S] and [4Fe–4S] clusters to effector apoproteins. The central components of both systems are cysteine desulfurases (IscS and SufS). These PLP (pyridoxal 5′-phosphate)-dependent enzymes convert L-cysteine into L-alanine leading to the release of a sulfur atom that forms a persulfide on a cysteine residue of the enzyme [7,8]. In the case of *E. coli* IscS, sulfur is transferred to the apo-form of the Fe–S scaffold protein IscU by protein–protein interaction leading to the formation of a [2Fe–2S] cluster in the presence of iron. Once two [2Fe–2S] clusters have been generated on an IscU dimer, an [4Fe–4S] cluster can be formed and transferred to Fe–S effector proteins or the A-type carrier protein IscA. This protein is believed to have a Fe–S cluster-delivery role. Release of IscU-bound Fe–S clusters involves the ATP-hydrolysing activity of the co-chaperones HscA and HscB [2]. The products of the stress-induced SUF operon are similar to those of the ISC-operon. They include a scaffold protein (SufB), an A-type carrier (SufA) and probably an ATPase (SufC) triggering the release of Fe–S clusters from SufB [2,3].

The considerable amount of knowledge available concerning Fe–S cluster biogenesis in Gram-negative bacteria is primarily based on observations made in ISC-knockout mutants. The phenotypes of these mutant strains clearly demonstrate the importance

Abbreviations: Acn, aconitase; ADC, albumin/dextrose/catalase; Ade, adenine; Ec, *Escherichia coli*; FdhF, formate dehydrogenase H; ISC, iron–sulfur cluster; MOI, multiplicity of infection; Mtb, *Mycobacterium tuberculosis*; Nfs1, NiFS-like 1; PLP, pyridoxal-5′-phosphate; ROS, reactive oxygen species; SD, synthetic defined; SdhB, succinate dehydrogenase; SirA, sulfite reductase; SUF, sulfur metabolism; trmU, tRNA 5-methylaminomethyl-2-thiouridylate methyltransferase; Y2H, yeast two-hybrid.

[1] To whom correspondence should be addressed (email jan.rybniker@epfl.ch).

Co-ordinates and structure factors for *Mycobacterium tuberculosis* IscS have been deposited in the PDB under accession code 4ISY.

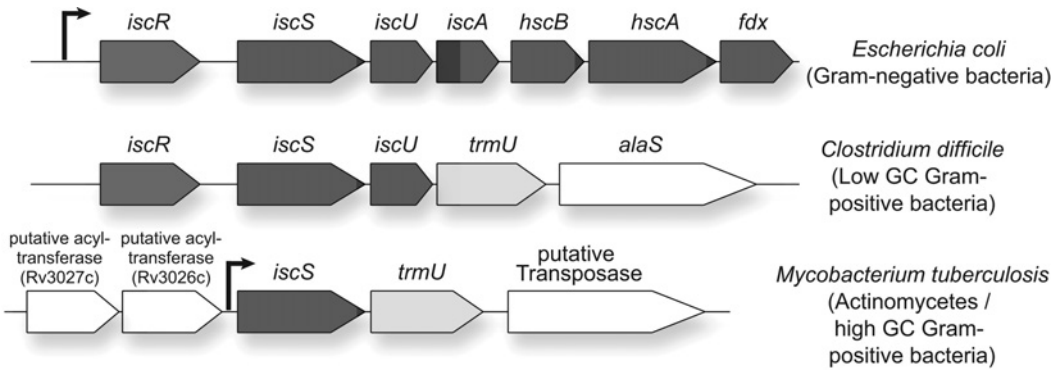

Figure 1 Comparison of ISC operons from different bacterial species

Genes involved in Fe–S cluster assembly are displayed in dark grey. The *E. coli* genome contains the full *iscRSUA-hscBA-fdx* operon which is found in most Gram-negative bacteria and serves as a prototype for scaffold-based Fe–S-cluster assembly through IscA/U after liberation of sulfur from L-cysteine by the cysteine desulfurase IscS. In low-GC-content Gram-positive bacteria, such as *C. difficile*, several assembly genes are missing. The non-Fe–S *trmU* gene, which is required for 2-thio-modification of some tRNAs, is the last gene of the operon. A very drastic change occurs in *M. tuberculosis* and most actinomycetes where the operon is composed of the *iscS* and *trmU* genes only. All Fe–S scaffold proteins, as well as the regulatory protein IscR, are missing, which initially led to the assumption that mycobacterial IscS is not involved in Fe–S-cluster assembly [13]. Through complementation studies performed on the Δ*iscS* strain generated in the present study, the presence of a putative promoter could be confirmed between Rv3026c and *iscS*.

of this operon under Fe–S cluster-damaging conditions. *E. coli* strains with defects in Fe–S cluster biogenesis are hypersensitive to H_2O_2 since Fe–S clusters are perturbed by stress conditions such as oxidative stress [8,9]. Furthermore, the deletion of *iscS* in *E. coli* leads to distinct alterations of growth rate under changing oxygen tensions and impaired activity of Fe–S cluster-dependent enzymes such as Acn (aconitase) [8]. These mutants were also used to show that IscS has been highly conserved during evolution, which facilitated heterologous complementation studies using IscS copies of different organisms [9–12]. It was thus shown that the slow-growth phenotype of an *E. coli* Δ*iscS* strain could be rescued by overexpressing the yeast IscS homologue Nfs1 (NiFS-like 1). Furthermore, IscSEc (where EC denotes *E. coli*.) complements the deleted *Nfs1* gene in yeast when expressed with a presequence that shuttles the protein to the mitochondrion [10,11].

The formation of Fe–S clusters and the role of cysteine desulfurases in Gram-positive bacteria are less well understood. We performed a genomic analysis revealing that most low-GC-content Gram-positive bacteria, such as *Clostridium difficile*, display a reduced ISC operon where genes such as *iscA* and the chaperones *hscA* and *hscB* are missing (Figure 1). In the actinomycete *Mycobacterium tuberculosis*, a Gram-positive bacterium with a high GC content, the reduction of the ISC operon is even more dramatic and only the gene coding for the cysteine desulfurase IscS (IscSMtb, where Mtb denotes *M. tuberculosis*; Rv number Rv3025c) is retained (Figure 1). Since *M. tuberculosis* contains a SUF operon comparable with those found in many other bacteria, it is not known whether IscSMtb is also involved in Fe–S cluster generation *in vivo* [13]. However, a conserved region around the active-site cysteine residue clearly indicates that IscSMtb is a group I (IscS-like) cysteine desulfurase [14]. Furthermore, it was shown previously that affinity-purified IscSMtb is capable of reconstituting the [4Fe–4S] cluster of WhiB3 *in vitro* [15,16]. WhiB3 belongs to a family of regulatory Fe–S proteins present only in actinomycetes and their bacteriophages [17–20].

The survival and spread of *M. tuberculosis* relies on the successful adaptation to extremely variable environments ranging from high oxygen tensions in the lung to hypoxic conditions in the granuloma. In addition, this intracellular pathogen encounters changing redox conditions inside and outside the macrophage. These rapidly changing environments require fine-tuned Fe–S cluster biogenesis and repair. Indirect evidence of a role for IscSMtb in the oxidative stress response is given by microarray data showing that *iscS* is up-regulated after exposure to nitric oxide and H_2O_2 [21]. To better understand the role of IscS in mycobacterial Fe–S cluster biogenesis we created a Δ*iscS*Mtb mutant which showed a phenotype strongly associated with impaired Fe–S cluster assembly. Since an IscU homologue is missing in the mycobacterial ISC operon, we tested for direct interaction of IscSMtb with mycobacterial Fe–S proteins. Intriguingly, we were able to identify an extensive IscS–Fe–S protein-interaction network. Repeating these assays with the well-described IscSEc instead of IscSMtb led to markedly different results. Finally, we provide structural data explaining the failure of IscSMtb to interact with IscU and the evolutionary deletion of this gene from the mycobacterial ISC operon.

We conclude that the mycobacterial IscS has a role in Fe–S cluster assembly and in combating oxidative stress, although the respective ISC operon does not imply such a role. In addition we show that the mycobacterial protein differs from IscS homologues found in eukaryotes and Gram-negative bacteria.

MATERIALS AND METHODS

Bacterial strains, culture conditions and cloning strategies

M. tuberculosis H37Rv was grown in 7H9 broth (Difco) supplemented with 0.2 % glycerol, Middlebrook ADC (albumin/dextrose/catalase) enrichment and 0.05 % Tween 80 or on solid Middlebrook 7H10 medium (Difco) supplemented with OADC (oleic acid/ADC). For selection, hygromycin, streptomycin and kanamycin were used at a concentrations of 50 μg/ml, 25 μg/ml and 20 μg/ml respectively and sucrose was used at a concentration of 5 %. Microaerophilic growth was performed using the GasPak™ pouch system from Becton Dickinson (EZ Campy system) or by overlaying *M. tuberculosis* colonies on 7H10 agar with 10 ml of top agar (7H9 medium with 0.75 % agar). H_2O_2 exposure was performed in 7H9 broth with 5 mM H_2O_2 for 3 h. *E. coli* BL21(DE3) cells were used for expression of His_6-tagged IscSMtb in LB medium containing 50 μg/ml ampicillin. All cloning steps were performed as described previously using the In-Fusion PCR Cloning kit (Clontech) [17]. Site-directed mutagenesis was performed

using the QuikChange II system (Agilent) according to the manufacturer's recommendations. For cytotoxicity assays, THP-1 macrophages were grown in RPMI 1640 medium supplemented with 10 % (v/v) FBS and activated with 200 nM PMA for 48 h. Cells were washed and infected with mycobacteria at an MOI (multiplicity of infection) of 5. MRC-5 fibroblasts were grown in MEM (minimal essential medium) supplemented with 10 % (v/v) FBS and seeded into 96-well plates at 20 000 cells per well. Cells were allowed to adhere and myocobacteria were added at an MOI of 10. After 24 h, extracellular bacteria were removed by washing with PBS and, after an additional 48 h of incubation in growth medium at 37 °C under 5 % CO_2, 10 % PrestoBlue® (Invitrogen) was added and the reaction was incubated for 1 h after measurement of fluorescence at 560/590 nm.

Allelic exchange and unmarked deletion of iscS

Details of the primers and plasmids used are shown in Supplementary Tables S1 and S2 (http://www.biochemj.org/bj/459/bj4590467add.htm). *M. tuberculosis* H37Rv cells were washed three times in 10 % (v/v) glycerol and transformed with pGA44:*iscS* followed by selection on 7H10 agar containing streptomycin. These clones were transformed with pJG:Rv3026/*trmU*, and positive clones were selected on 7H10 agar containing hygromyin and kanamycin. Clones containing both plasmids were plated on 7H10 agar with streptomycin and sucrose. The deletion of *trmU* (tRNA 5-methylaminomethyl-2-thiouridylate methyltransferase) was performed using pJG:Rv3023/iscS.

DNA extraction and Southern blot analysis

Mycobacteria were treated overnight at 37 °C with SET buffer [25 % sucrose, 50 mM sodium EDTA and 50 mM Tris/HCl (pH 8)] containing 3 mg/ml lysozyme. After the addition of RNase (subsequent incubation at 37 °C for 30 min) and proteinase K (subsequent incubation 55 °C for 30 min) DNA was extracted with phenol/chloroform and ethanol-precipitated. For Southern blot analysis, 4 μg of DNA was digested with AclI and AvrII and separated by agarose gel electrophoresis. After denaturation the DNA was blotted on to a Hybond N+ membrane. For probe labelling and detection the ECL direct nucleic acid labelling and detection kit (GE Healthcare) was used following the manufacturer's recommendations. A PCR product spanning Rv3026/*trmU* without *iscS* was used as the probe.

RNA extraction and PCR

For gene expression analysis, RNA was extracted with TRIzol® (Invitrogen) and treated with DNase I (Roche) before generation of the cDNA template. cDNA was synthesized using the RevertAid First Strand cDNA Synthesis kit (Fermentas) using random hexamer primers. cDNA corresponding to 10 ng of input RNA was used in each RT (reverse transcription)–PCR supplemented with specific primer pairs (200 nM each) listed in Supplementary Table S2 and SYBR Green Master mix (Applied Biosystems). qPCR (quantitative real-time PCR) was performed with the 7900HT Fast Real-Time PCR system (Applied Biosystems) with the following parameters: 50 °C for 2 min and 95 °C for 10 min, followed by 40 cycles of 95 °C for 15 s and 60 °C for 60 s. Melt curve analysis was used to confirm specific amplification of each primer pair.

Y2H (yeast two-hybrid) assays

The Matchmaker Gal4 Two-hybrid System 3 (Clontech) was used to screen for proteins that interact with IscSMtb and IscSEc. The respective plasmids based on pGBKT7 and pGADT7 (Supplementary Table S1) were co-transformed into yeast strain AH109 according to the recommendations of the manufacturer. Transformants were plated on SD (synthetic defined) minimal medium (− Leu/ − Trp) and subcultured on high stringency plates [SD/ − Ade (adenine)/ − His/ − Leu/ − Trp/X-α-galactosidase].

Purification of His_6-tagged IscSMtb

Mid-exponential-phase culture (2 litres) was induced with 0.5 mM IPTG and incubated for 12 h at 16 °C. *E. coli* BL21(DE3) cells were lysed in lysis buffer [50 mM Tris/HCl (pH 8), 500 mM NaCl, 5 mM imidazole, 10 % (v/v) glycerol and 1 % (w/v) Tween 20] using a French press. After clearance by centrifugation, the lysates were incubated with 1 g of PrepEase resin (USB) for 1 h at 4 °C followed by separation on a PolyPrep chromatography column (Bio-Rad Laboratories). The resin was washed with two column volumes of buffer containing 10 mM imidazole and eluted with 250 mM imidazole. After dialysis against 25 mM Tris/HCl (pH 7.5) and 100 mM NaCl the protein was further purified by gel filtration on a HiLoad 16/60 Superdex 200 column (GE Healthcare).

Pull-down experiments

Experiments were performed with S-tagged WhiB3, Acn or ShdB expressed from pETduet-1 as prey and His-tagged IscSMtb expressed from pQE80 as bait. Empty pQE80 was used as a negative control. *E. coli* BL21(DE3) cultures (500 ml) were grown and induced as described above. Prey and bait cultures were mixed, and lysis and resin binding were performed as described above [lysis buffer: 25 mM Tris/HCl (pH 8), 200 mM NaCl, 5 mM imidazole and 2 % (v/v) glycerol]. After elution with lysis buffer containing 250 mM imidazole, proteins were separated by SDS/PAGE (4–12% gel) and transferred on to a nitrocellulose membrane. S-tagged proteins were detected using an S-tag monoclonal antibody at a dilution of 1:5000 (Merck).

Enzyme assays

Enzyme assays with L-cysteine as substrate contained 200 mM Tris/HCl (pH 7.5), 50 mM NaCl, 0.25 mM PLP and 0.5–100 mM L-cysteine dissolved in water and 5 mM DTT. Before enzyme assays for determining the activity of IscS with L-selenocysteine were performed, L-selenocystine had to be reduced to obtain L-selenocysteine. For this purpose L-selenocystine was first solved in a water/methanol (1:2, v/v). Subsequently, the pH was increased by the addition of two equivalents of a 1 M NaOH solution while cooling on ice. $NaBH_4$ was added in portions under stirring until the yellow mixture became colourless. The pH was adjusted to pH 5.5 to obtain the free amino acid instead of the sodium salt. The L-selenocysteine assay mixtures contained 200 mM Tris/HCl (pH 7.5), 50 mM NaCl, 0.25 mM PLP and 3.75–30 mM L-selenocysteine. The enzyme assays were started by the addition of purified protein (100 μg in 1 ml) and were performed at 37 °C. Several 50 μl samples were collected over a period of 20 min, and reactions were terminated by mixing each sample with 30 μl of 5 % perchloric acid and 38 % ethanol. After neutralization with 20 μl of 20 mM Tris/HCl (pH 8) buffer containing 23 mM K_2CO_3, the precipitated salts were removed by centrifugation (16 200 ***g*** for 10 min at 22 °C). Subsequently, the product, L-alanine, was quantified by ultra-high-pressure liquid chromatography as its *o*-phthaldehyde derivative. Assays were linear over time and proportional to the protein concentration applied.

For Acn activity, exponentially growing cultures were lysed by beadbeating with 0.1 mm zirconia beads in ice-cold assay buffer. After centrifugation (16200 ***g*** for 10 min at 4 °C), Acn activity was measured in the supernatant in a coupled enzymatic reaction using an Acn activity assay kit (Sigma–Aldrich). SdhB (succinate dehydrogenase) activity was measured according to the method of Munujos et al. [22]. Whole-cell lysates (10 μl; 200 ng/μl total protein) were added to 90 μl of reaction buffer in a 96-well plate and colour development was monitored at 500 nm in a Tecan M200 microplate reader at 30 °C.

Protein crystallization and X-ray data collection

Approximately 1000 buffer conditions were screened for protein crystals with 10 mg/ml IscSTB in 25 mM Tris/HCl (pH 7.5) and 100 mM NaCl. The best condition was refined using the hanging-drop vapour-diffusion method in drops of 2–4 μl at 18 °C. Diffraction-quality crystals were grown in a crystallization solution consisting of 0.2 M ammonium sulfate, 0.1 M Bis-Tris (pH 5.5), 10 % (w/v) PEG 3350 and 5 % (v/v) glycerol. All crystals were cryoprotected in reservoir mother liquor supplemented with 25 % (v/v) glycerol and directly flash-cooled in liquid nitrogen. Diffraction data were collected on beamlines PXII and PXIII of the Swiss Light Source (Villigen, Switzerland). All data were indexed, scaled and integrated using XDS [23].

Structure determination and model refinement

IscSMtb was crystallized in the P_1 space group with unit cell dimensions of approximately $a = 66$ Å (1 Å = 0.1 nm), $b = 78$ Å, $c = 93$ Å, $\alpha = 94°$, $\beta = 104°$ and $\gamma = 99°$, with four molecules in the asymmetric unit. Phase determinations were carried out by molecular replacement using Phaser [24], part of the CCP4 Suite [25]. IscSMtb was modelled on the published structure of IscS from *E. coli* [36] with PDB code 3LVM used as search model. The initial molecular replacement models were manually adjusted in COOT, part of the CCP4 Suite [25], and refined with REFMAC5 [26]. Structure figures were prepared with PyMOL (http://www.pymol.org). All crystallographic statistics are listed in Supplementary Table S3 (http://www.biochemj.org/bj/459/bj4590467add.htm). Co-ordinates and structure factors for IscSMtb have been deposited in the PDB under accession code 4ISY.

LC–MS/MS

An FDR (false discovery rate) of 1 %, a minimum peptide Mascot score of 25 and a minimum of two matching peptides per protein were used as the identification criteria for Mtb proteins. A normalized spectrum count was used to compare the relative abundance of proteins. A detailed description of the LC–MS/MS methods used in the present study can be found in the Supplementary Online Data (http://www.biochemj.org/bj/459/bj4590467add.htm).

RESULTS

The Δ*iscS*Mtb mutant is microaerophilic, hypersensitive to H_2O_2 stress and displays impaired activity of Fe–S cluster-dependent enzymes

The *iscS* gene of *M. tuberculosis* was predicted to be essential for cell viability by high-density mutagenesis [27]. To create an unmarked deletion we first complemented *M. tuberculosis* H37Rv with pGA44:*iscS*, a plasmid carrying a tetracycline-repressible pristinamycin-dependent promoter. We then deleted *iscS* using pJG:Rv3026/*trmU* which contains the genes flanking *iscS* and the *sacB* gene for counterselection. After selection on medium containing sucrose, successful allelic exchange was confirmed by Southern blotting (Figure 2A). Compared with the wild-type strain, the growth rate of the complemented Δ*iscS* strain was slightly lower and the addition of tetracycline led to a pronounced deceleration of growth (Figure 2B). However, even in the presence of tetracycline, there was observable growth allowing the conclusion that IscS is not fully essential. To confirm this we performed a second deletion using pJG:Rv3026/*trmU* on a wild-type background. After counterselection, small colonies were visible after 10 weeks of incubation at 37 °C and the successful deletion of *iscS* was confirmed by PCR (results not shown). Complementation of this mutant was possible with both plasmids expressing IscS from the strong *HSP60* (heat-shock protein 60) promoter (pMV261B:*iscS*Mtb) or from the putative endogenous promoter upstream of *iscS* (pMD31:*iscS*Mtb). Incubating the mutant strain for 3 months revealed a distinct smooth and ruffled colony morphology which could be converted into the typical rough and spread-out colony morphology of wild-type *M. tuberculosis* upon complementation with *iscS* (Figure 2C). Interestingly, it was reported previously that a *whiB3*-knockout mutant showed similar colony morphology, and a defect in cord formation appears to be a feature of both mutants [15]. These data show that *iscS* is not essential on rich medium, but its deletion leads to a slow-growth phenotype and altered morphology. When subcultured several times in liquid medium the growth rate could be increased and finally reached H37Rv wild-type levels. However, when these bacteria were plated on solid medium, the growth rate was again heavily reduced and the colonies were smooth, indicating a stable phenotype.

The generation of the Δ*iscS*Mtb mutant allowed us to identify characteristics associated with a putative role of IscS in Fe–S cluster assembly. Incubation of wild-type, knockout and complemented knockout mutant *M. tuberculosis* cells with 5 mM H_2O_2 for 3 h showed increased sensitivity of the mutant strain towards oxidative stress (Figure 3A). Further proof of a role for IscS in protecting *M. tuberculosis* from oxidative stress was obtained on overexpression of the protein from the strong pristinamycin-dependent promoter as this rendered the cells resistant to H_2O_2 (Figures 3A and 3B).

To test whether the deletion of *iscS*Mtb leads to altered activity of Fe–S cluster-dependent enzymes we quantified Acn activity in mycobacterial whole-cell lysates (Figure 3C). The [4Fe–4S] cluster of this TCA (tricarboxylic acid) cycle enzyme is essential for the conversion of citrate into isocitrate. Compared with the wild-type strain, the Δ*iscS*Mtb mutant displayed approximately 50 % less Acn activity, which is comparable with the activity seen in the Δ*iscS* mutant of *E. coli* [8]. Acn activity could be restored through complementation (Figure 3C). Equal total amounts of Acn were identified by LC–MS/MS in the examined whole-cell lysates, ruling out reduced enzymatic activity due to different amounts of enzyme (Supplementary Figures S1A and S1B at http://www.biochemj.org/bj/459/bj4590467add.htm). We also tested for activity of the Fe–S protein SdhB in the respective strains. This enzyme also showed impaired activity in the mutant (Supplementary Figure S1C).

The biogenesis of Fe–S clusters is sensitive to oxygen since iron and sulfide can be modified by oxygen or ROS (reactive oxygen species), eventually leading to cluster decay. When grown under microaerophilic conditions, the growth rate of the mutant could be enhanced and was almost comparable with that of the H37Rv wild-type strain grown under the same conditions, indicating that IscS is needed for cluster assembly or repair under normal oxygen conditions (Figure 3D).

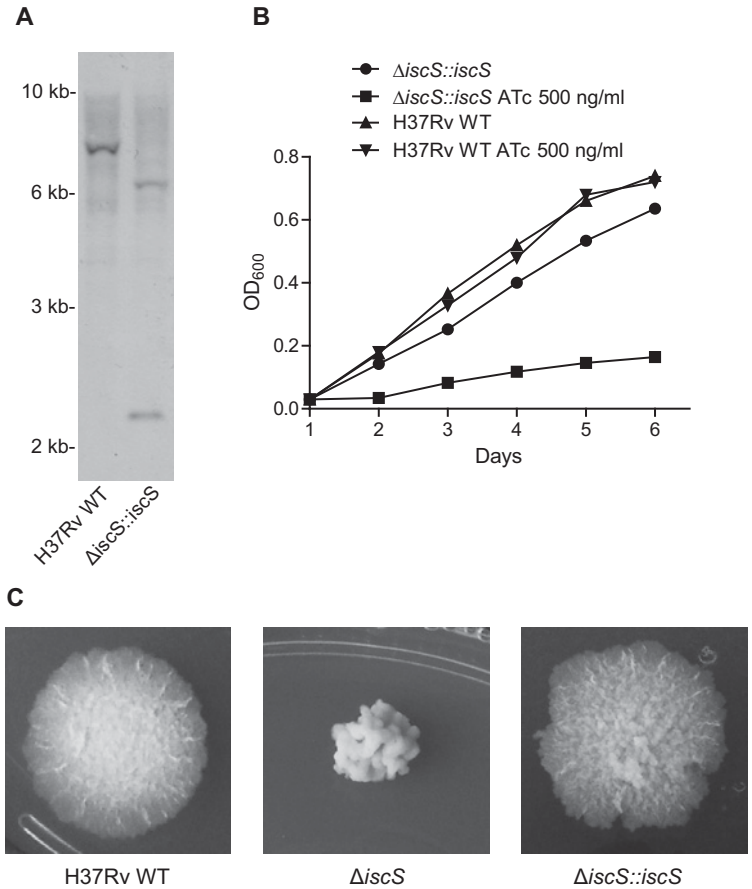

Figure 2 Unmarked deletion of *iscS* in *M. tuberculosis*

(**A**) Southern blot of *M. tuberculosis* H37Rv (wild-type) and complemented Δ*iscS::iscS* DNA digested with AclI and AvrII. The latter site was genetically engineered between the flanking *iscS* genes leading to the formation of two detectable DNA fragments of approximately 1.9 and 6.3 kb in the mutant and only one fragment of 8.2 kb in the wild-type. The *iscS* flanking genes served as the probe. (**B**) Growth curves of *M. tuberculosis* H37Rv and Δ*iscS::iscS* strain with and without anhydrous tetracycline (ATc). Down-regulation of IscS through anhydrous tetracycline leads to slower, but detectable, growth. OD_{600}, attenuance at 600 nm. (**C**) Colony morphology of *M. tuberculosis* H37Rv, mutant and complemented Δ*iscS* strain after incubation for 3 months. The Δ*iscS* strain shows small colonies that have a smooth and ruffled colony morphology compared with the wild-type and complemented strains.

Putative targets of IscSMtb are Fe–S proteins with important roles in the virulence of *M. tuberculosis*. Furthermore, phagocytosis shifts the bacteria into redox-active cell compartments, which are dedicated to the elimination of microbes. We thus tested the Δ*iscS* strain in THP-1 macrophage and MRC-5 lung fibroblast virulence assays. At an MOI between 5 and 10, wild-type *M. tuberculosis* is cytotoxic for activated macrophages as well as fibroblasts and this can be quantified using cell viability assays [28,29]. After 72 h of infection, the Δ*iscS* strain was significantly less cytotoxic for macrophages and fibroblasts than the H37Rv wild-type or the complemented mutant strain, indicating an attenuated phenotype *in vitro* (Figure 3E).

It was shown recently that the deletion of *trmU* has an effect on the intracellular redox state of *E. coli* [30]. To rule out the possibility that the phenotype we observed for the Δ*iscS* strain was not due to impaired TrmU activity as a consequence of insufficient sulfur transfer, we deleted *trmU* in *M. tuberculosis* (Supplementary Figure S2A at http://www.biochemj.org/bj/459/bj4590467add.htm) and performed Acn- and H_2O_2-sensitivity assays. The Δ*trmU* strain performed like wild-type *M. tuberculosis* in both assays indicating that the impaired Fe–S protein activity we observed in the Δ*iscS* strain is independent from TrmU (Supplementary Figures S2B and S2C).

Complementation with *iscS* of *E. coli* does not rescue the small colony morphology or Acn activity of the Δ*iscS*Mtb mutant

The high conservation of *iscS* genes allowed for successful heterologous complementation experiments in *iscS* mutants of several organisms [10–12]. In order to identify distinct features of the mycobacterial protein we also tried to complement the Δ*iscS*Mtb strain by overexpressing the well-described IscS protein of *E. coli* from a mycobacterial promoter. However, we were not able to rescue the small colony morphology of the knockout strain (Figure 4A). This failure for complementation was not due to low transcription or expression levels of IscSEc since we were able to detect and quantify the protein by LC–MS/MS in the mycobacterial cytosol (Figure 4B). We also tested for Acn activity in this IscSEc complemented mutant. Expression of IscSEc did not restore the full activity of the enzyme (Figure 3C).

IscSMtb uses both L-cysteine and L-selenocysteine as substrates

To rule out differences in enzyme kinetics as a possible explanation for the failure of IscSEc in complementing Δ*iscS*Mtb, we assayed for cysteine desulfurase activity of recombinant IscSMtb. So far IscSMtb cysteine desulfurase activity was only

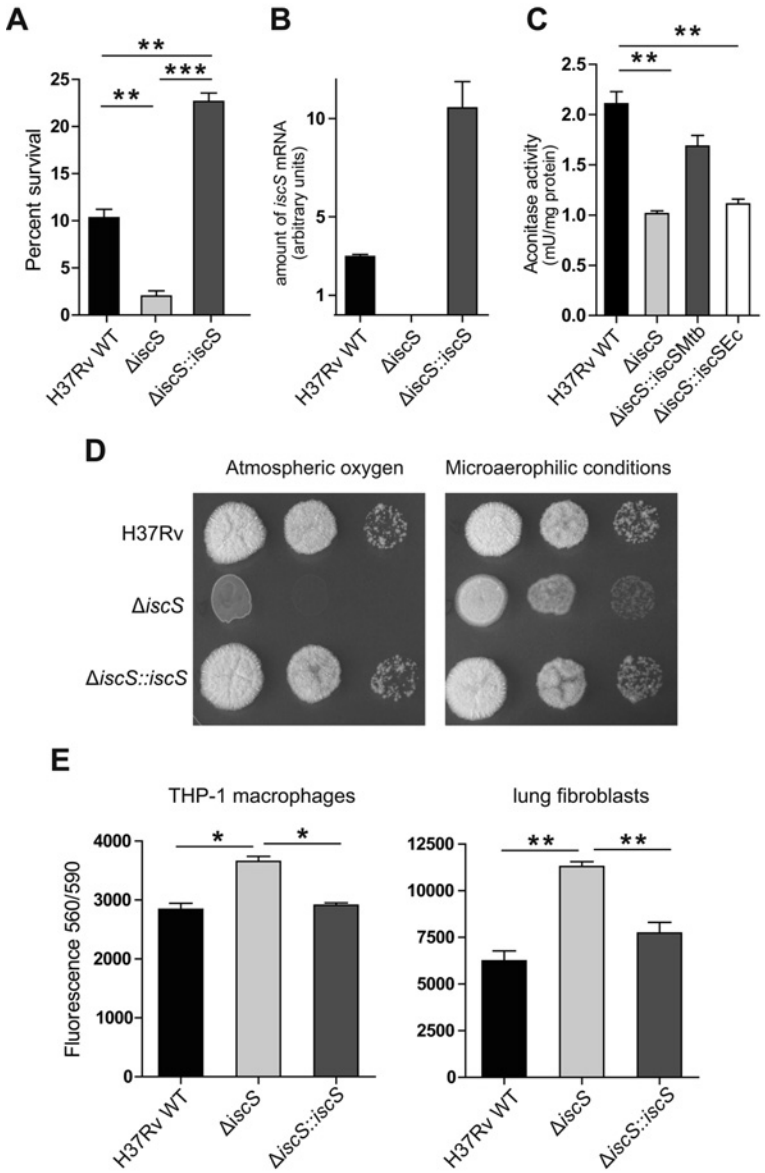

Figure 3 Growth characteristics of Δ*iscS* under various conditions and cytotoxicity assays

(**A**) Mycobacteria were exposed to 5 mM H_2O_2 and serial dilutions were plated before and after exposure. Colony-forming units (cfu) were counted after 4 weeks of incubation (wild-type strain and complemented mutant) or after 3 months of incubation (Δ*iscS* mutant). The knockout is more sensitive to H_2O_2, whereas overexpression of IscS protects from oxidative stress. (**B**) *IscS* mRNA levels of the three strains correlate with survival during H_2O_2 exposure. Expression of IscSMtb from the pristinamycin-dependent promoter leads to higher levels of IscS-specific mRNA compared with *IscS* mRNA levels of the wild-type strain. (**C**) Acn activity of whole cell lysates; the Δ*iscS* mutant shows significantly less activity than wild-type and complemented mutant. Complementation with IscSEc did not restore enzymatic activity. (**D**) Growth of the Δ*iscS* strain is enhanced under microaerophilic conditions. Serial dilution (10-fold) of individual strains were spotted on 7H10 agar plates and incubated under different growth conditions. (**E**) Activated THP-1 macrophages and MRC-5 lung fibroblasts were infected with mycobacteria at an MOI of 5 (macrophages) or 10 (fibroblasts). Cells were incubated for 3 days and viability was measured by the addition of PrestoBlue® and subsequent determination of fluorescence at 560/590 nm. The deletion of *iscS* leads to better survival of the eukaryotic cells indicating impaired virulence of the knockout strain *in vitro*. Results are means ± S.E.M. (unpaired two-tailed Student's *t* test). $^{***}P \leqslant 0.001$, $^{**}P = 0.01$ and $^{*}P < 0.05$.

shown indirectly by a shift of its UV–visible spectrum after the addition of L-cysteine [16]. We quantified the product L-alanine after the addition of different concentrations of L-cysteine to the affinity-purified IscSMtb. Assuming Michaelis–Menten kinetics, we determined a K_m value of 6.1 mM (Figure 4C) and, at a concentration of 12 mM L-cysteine, a specific activity of 0.31 μmol/min per mg, which is similar to previously published data on IscSEc [31]. Several cysteine desulfurases, including IscSEc, were shown to provide selenium for selenoproteins such as FdhF (formate dehydrogenase H) and selenium-containing tRNAs using L-selenocysteine as a substrate [32]. We were interested in similar activity for IscSMtb and performed enzymatic assays with this substrate. L-selenocysteine was generated from reduced L-selenocystin as described in the Materials and methods section. We were able to identify a high specific activity for this substrate at a concentration of 7.5 mM L-selenocysteine (Figure 4D). At higher concentrations, enzyme activity was decreased most probably due to acidification of the reaction buffer by the substrate, which has a pH of 5.5 (results not shown). However, we could clearly show that IscSMtb is capable of using both L-cysteine and L-selenocysteine as substrates. These data indicate that, despite similar enzymatic activities, IscSMtb is

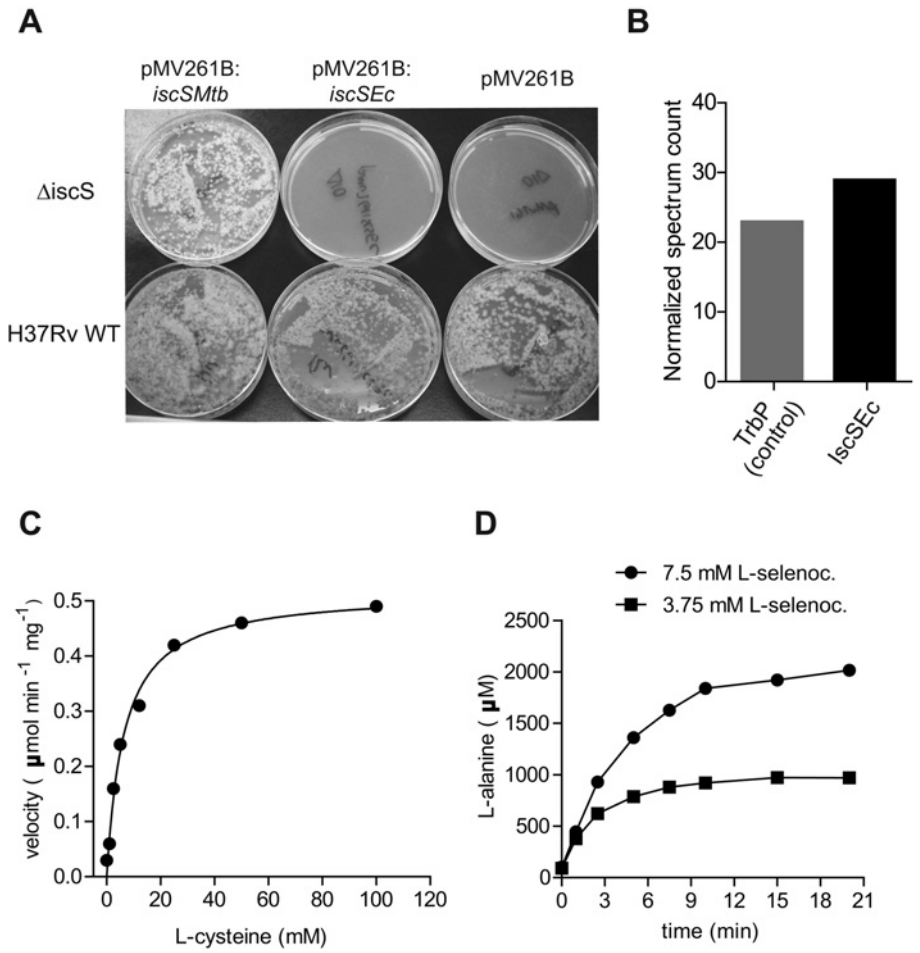

Figure 4 Complementation of Δ*iscS* with *iscS* from *M. tuberculosis* or *E. coli*

(**A**) Individual plasmids were transformed in the Δ*iscS* strain or H37Rv wild-type and incubated for 6 weeks. Expression of IscSMtb restored normal growth in the mutant, whereas expression of IscSEc leads to the same slow-growth phenotype seen in the mutant transformed with the empty vector (pMV261B). (**B**) Quantification of IscSEc expressed in *M. tuberculosis*. Proteins of the cell lysate were separated by SDS/PAGE and the band at 45 kDa was examined by LC–MS/MS as described in the Materials and methods section. The mycobacterial tryptophan synthase TrbP was identified and quantified in the same gel slice and functions as a control protein of comparable mass. Representative data from three individual experiments are shown. (**C**) Michaelis–Menten kinetics of IscSMtb with L-cysteine as substrate. (**D**) Time-dependent conversion of L-selenocysteine into L-alanine by IscSMtb.

functionally distinct from its *E. coli* counterpart upon expression in the mycobacterial host.

IscSMtb, but not IscSEc, interacts with several mycobacterial Fe–S and sulfur-accepting proteins

An intracellular excess of free iron and sulfur is toxic for most bacteria and eukaryotes. Thus, in the IscS proteins examined so far, sulfur is liberated from cysteine and transferred to the scaffold protein IscU [33]. Since an IscU homologue is absent from the mycobacterial ISC operon, we were interested in the direct interaction of IscSMtb with putative sulfur-accepting Fe–S proteins. IscSMtb is capable of reconstituting the [4Fe–4S] cluster of apo-WhiB3, a mycobacterial transcriptional regulator, *in vitro* [16]. Using Y2H assays we were able to show an interaction of both proteins (Figure 5A). Furthermore, interactions were identified for other known Fe–S protein targets of the ISC system, such as the enzymes Acn (Rv number Rv1475c), SdhB (Rv number Rv3319), FdhF (Rv number Rv2900c) and the SirA (sulfite reductase; Rv number Rv2391). In addition, IscSMtb interacts with the non-Fe–S protein and mycobacterial ISC operon member TrmU (Figure 5A). Y2H assays were repeated with switched vectors in which IscSMtb was fused to the binding domain of the reporter system (pGBKT7-IscSMtb) and mycobacterial Fe–S proteins to the activating domain of the reporter plasmid pGADT7. These experiments gave identical results (not shown; see Supplementary Table S1 for the plasmid constructs).

Protein interactions identified in the Y2H experiments were confirmed for three mycobacterial Fe–S proteins (WhiB3, Acn and SdhB) by *in vitro* pull-down experiments. S-tagged Fe–S proteins overexpressed in *E. coli* were bound to His-tagged IscSMtb and captured on nickel resin. Protein complexes could be identified after immunoblotting and detection with an anti-S-tag antibody (Figure 5B).

To identify reasons for the failure of IscSEc to rescue the small colony phenotype of Δ*iscS*Mtb we repeated the Y2H experiments using IscSEc. First, we confirmed published experiments on the positive interaction of IscSEc with IscUEc indicating that our Y2H assay can be used to test for putative protein interactions of IscSEc with Fe–S proteins [33] (Table 1). When IscSEc was tested for interaction with mycobacterial Fe–S proteins, a positive result could only be obtained for IscSEc and WhiB3. In contrast

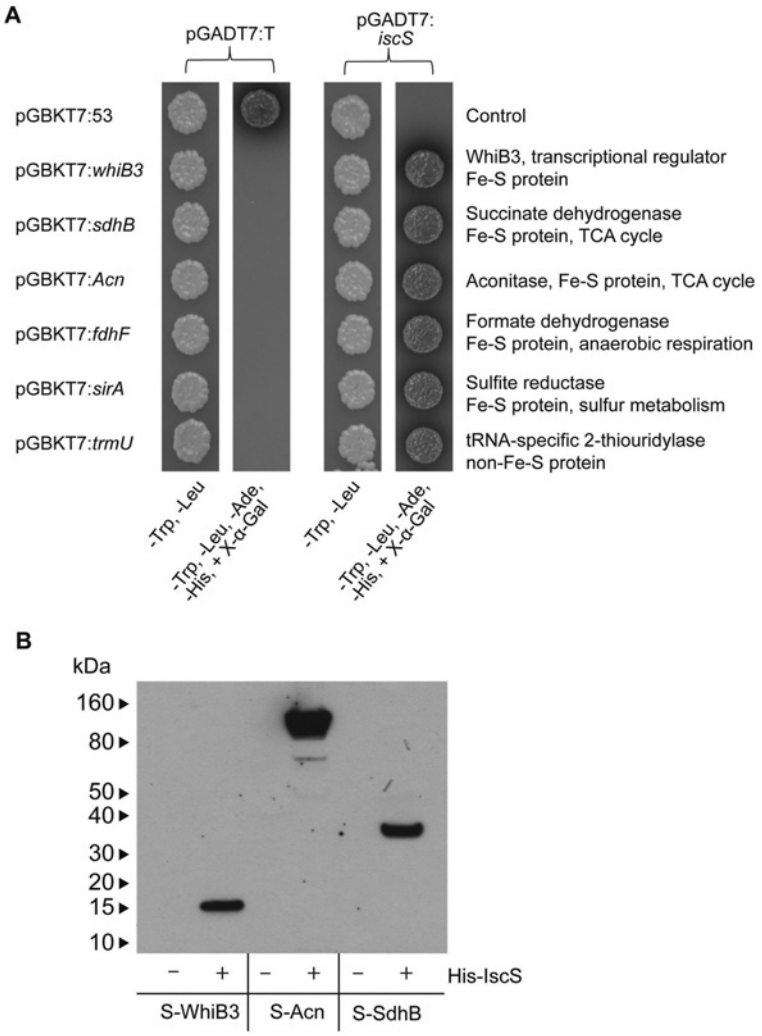

Figure 5 IscSMtb interacts with several mycobacterial Fe–S proteins

(**A**) Individual plasmids were co-transformed into yeast cells and plated on SD/ – Leu/ – Trp and SD/ – Ade/ – His/ – Leu/ – Trp media. All transformants grew well on SD/ – Leu/ – Trp plates showing successful co-transformation of plasmids. When subcultured on SD/ – Ade/ – His/ – Leu/ – Trp/ X-α-galactosidase medium, only the positive interaction of IscSMtb with mycobacterial proteins and subsequent transcription of reporter genes allows for growth of the auxotrophic yeast strain. Gal4 activation through protein–protein interaction leads to the development of blue-coloured (dark in the Figure) colonies giving further proof of robust association of IscSMtb with Fe–S proteins. IscSMtb strongly interacts with several mycobacterial Fe–S proteins and with the non-Fe–S protein TrmU. pGADT7:T and pGBKT7:53 are positive control vectors that contain the SV40 large T-antigen and the murine p53 protein, which strongly interact in Y2H assays. (**B**) *In vitro* pull-down experiments with S-tagged SdhB, Acn and WhiB3. Overexpressed proteins were bound to His-tagged IscSMtb and captured on nickel resin. Protein complexes were identified after immunoblotting and detection with an anti-S-tag antibody.

with IscSMtb, IscSEc failed to interact with SdhB, SirA and Acn. Thus the negative complementation phenotype that we observed for the Δ*iscS*Mtb::*iscS*Ec strain could be due to failure of IscSEc in interacting with sulfur-accepting proteins of *M. tuberculosis*.

We also tested for interaction of IscSMtb with IscU of *E. coli*. Although IscSMtb interacts with several mycobacterial Fe–S proteins, an interaction with this central sulfur-accepting protein of Gram-negative bacteria was not detectable (Table 1). The mycobacterial SUF operon contains an IscU/NifU-like gene product (Rv1465) with 24 % homology with the respective *E. coli* protein. This protein also failed to interact with IscSMtb (Table 1). The reason for these negative results could be a C-terminal α-helix absent from IscSMtb, a part of the protein that is mandatory for the IscS–IscU interaction in *E. coli* (see the structural data below) [34,35]. Of note, not only IscSMtb, but also the Fe–S acceptor protein WhiB3, failed to interact with the putative IscU/Rv1465 protein (Table 1).

Overall protein fold and active site are conserved in IscSMtb and IscSEc

To better define the distinct characteristics of the IscSMtb protein we crystallized the protein and solved the structure at 2.6 Å resolution. The crystallographic data collection statistics are given in Supplementary Table S3. As expected, IscSMtb forms a homodimer with the typical large and small domains seen in most PLP-dependent enzymes (Supplementary Figure S3 http://www.biochemj.org/bj/459/bj4590467add.htm) [36].

IscSMtb and IscSEc share similar secondary structure and topology except for a C-terminal α-helix absent from IscSMtb as shown by superimposition of the structures in Figure 6(A). Residues of the C-terminal α-helix were shown previously to be essential for the IscS–IscU interaction in *E. coli* [34,35].

In its active-site pocket, IscS catalyses the desulfuration of cysteine yielding alanine. This involves the formation of a Schiff

Table 1 IscSEc interacts with IscUEc, but not with the mycobacterial SdhB, SirA or Acn

Individual plasmids were co-transformed into yeast cells and plated on SD/ – Leu/ – Trp and SD/ – Ade/ – His/ – Leu/ – Trp media. As all transformants grew well on SD/ – Leu/ – Trp plates, the Table displays growth phenotypes of co-transformants after subcultivation on SD/ – Ade/ – His/ – Leu/ – Trp medium. IscSEc failed to interact with mycobacterial Fe–S proteins except for WhiB3. Additionally, IscSMtb failed to interact with the scaffold protein IscUEc, the major acceptor of IscS-derived sulfur in Gram-negative bacteria, and IscSMtb did not interact with Rv1465, a mycobacterial IscU/NifU homologue which is part of the SUF operon. pGADT7:T and pGBKT7:53 are positive control vectors that contain the SV40 large T-antigen and the murine p53 protein which strongly interact in Y2H assays. +, growth; –, no growth; nd, not determined.

Vector	pGBKT7:*IscU*Ec	pGBKT7:*whiB3*	pGBKT7:*sdhB*	pGBKT7:*Acn*	pGBKT7:*sirA*	pGBKT7:*IscS*Mtb	pGBKT7:53
pGADT7:*iscS*Ec	+	+	–	–	–	nd	–
pGADT7:*iscS*Mtb	–	+	+	+	+	nd	–
pGADT7:*Rv1465*	nd	–	nd	nd	nd	–	–
pGADT7:T	–	–	–	–	–	–	+

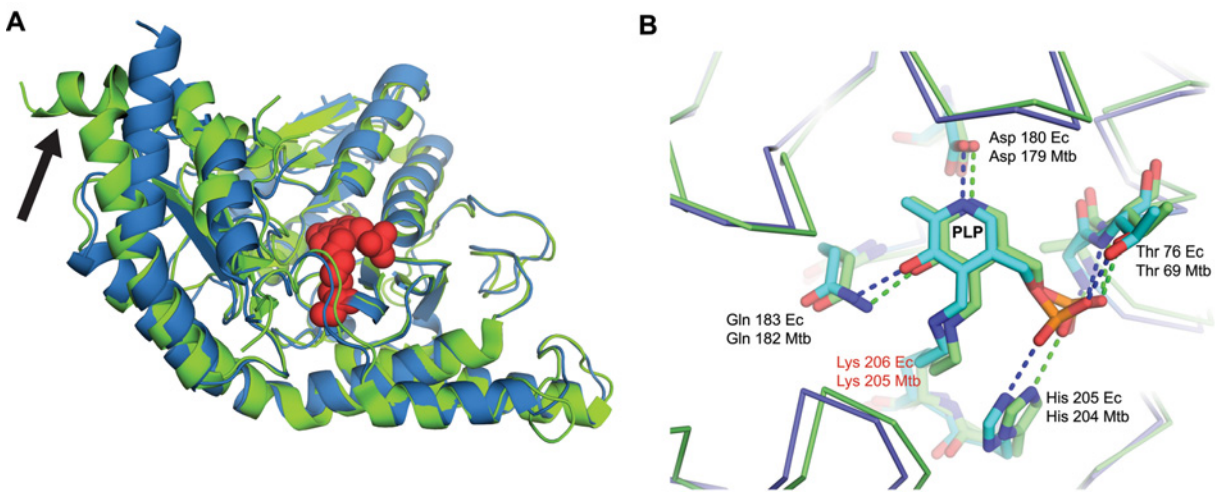

Figure 6 Structural alignment of IscSMtb (blue) and IscSEc (green) monomers

(**A**) Both proteins share a similar secondary structure and topology except for the most C-terminal helix of IscSEc which is missing in IscSMtb (black arrow). The PLP cofactor is displayed in red. (**B**) Magnified view of the PLP cofactor in the highly conserved active-site pocket. Ec, *E. coli*.

base between the substrate cysteine residue and the cofactor PLP followed by nucleophilic attack of the bound cysteine residue by Cys^{329} in IscSMtb and Cys^{328} in IscSEc. The highly homologous pockets of both proteins are rich in charged and/or polar amino acid side chains. The PLP group is anchored via an internal Schiff base with Lys^{205} in *M. tuberculosis* and Lys^{206} in *E. coli* (Figure 6B), and further stabilized by hydrogen bonds with identical amino acids in both enzymes indicating similar substrate-binding and catalysis mechanisms. Key to the versatile sulfur transfer activity of IscS proteins is the dual role of the active-site cysteine, which participates in catalysis of sulfur from the substrate cysteine and in transfer of a subsequently bound persulfide to effector proteins. The active-site cysteine residue is organized in a large and flexible loop, which does not display electron density in either the IscSEc structure (Cys^{328}–Lys^{333}) or our IscSMtb structure (Cys^{329}–Ala^{334}). However, the loop flanking amino acids, which are believed to ensure the necessary flexibility of the IscS loop, are conserved in both proteins, again indicating similar sulfur transfer mechanisms.

The surface amino acid composition of IscSMtb and IscSEc are highly distinct

Since IscSEc partially failed to interact with mycobacterial Fe–S proteins, we tested for differences in the properties of surface amino acids of the two IscS proteins using the Chimera software [37]. Interestingly, the electrostatic surface potential is dramatically different in large areas of the proteins (Figure 7), which is mirrored by net charge calculations of −34 e for IscSMtb and −12 e for IscSEc. This is most pronounced in the vicinity of the IscSMtb active site, where large patches of the protein display a negative charge which is not the case for IscSEc. Intriguingly, the polarity of the surface amino acids is much more conserved in the two proteins with predominantly hydrophilic side chains as expected for cytosolic proteins. IscSMtb shows only a slightly higher content of hydrophobic areas as shown in Supplementary Figure S4 (http://www.biochemj.org/bj/459/bj4590467add.htm).

The N-terminal part of IscSMtb is essential for protein–protein interactions

To map interaction domains of IscSMtb with sulfur-accepting proteins we performed deletion-mapping experiments of the C-terminus and probed these shorter versions of the protein in Y2H assays. It was found that large parts of the C-terminus could be deleted without affecting protein–protein interactions. However, putative regions between amino acids 68 and 143 are essential for interaction (Supplementary Figure S5A (http://www.biochemj.org/bj/459/bj4590467add.htm). This N-terminal part of IscSMtb is rich in arginine and tryptophan residues and a unique $WXRRX_5RRRX_{16}W$ motif can be found in IscS proteins of actinomycetes, but not in proteins of other Gram-positive or Gram-negative bacteria (Supplementary Figure S5A). The arginine residues of the two IscS monomers form a large

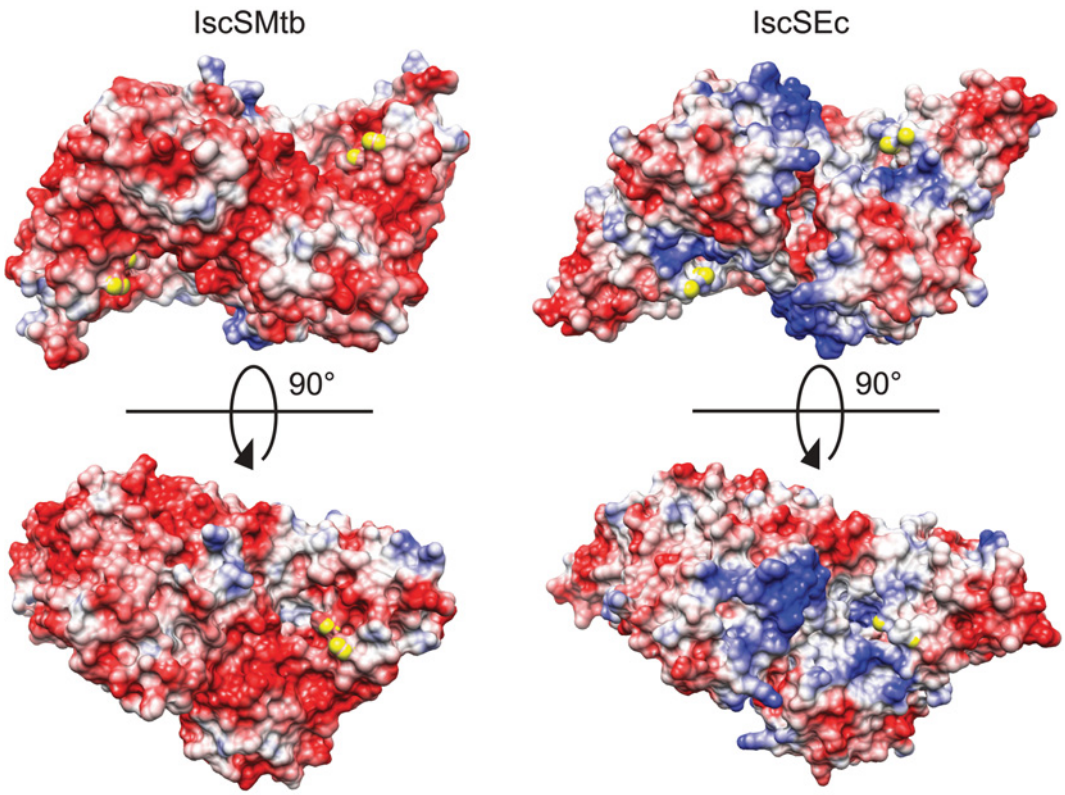

Figure 7 The electrostatic potential of the IscSMtb and the IscSEc dimer

Negatively charged amino acids prevail on the IscSMtb surface which is the opposite for IscSEc. The approximate position of the active-site loop, which does not show electron density in both structures, is displayed by yellow labelling of the loop flanking the N- and C-terminal amino acids. Red, negative charge; blue, positive charge.

surface-exposed hydrophilic patch, whereas two tryptophan residues of each monomer come together in a cleft formed by the dimer interface (Supplementary Figures S5B and S5C). The structural composition of this part of the mycobacterial protein is clearly distinct from its *E. coli* counterpart where interaction-sensitive arginine residues are primarily found towards the C-terminus [38]. In an attempt to identify the surface amino acids that are essential for proper IscSMtb function and protein–protein interaction, we performed structure-guided alanine-scanning mutagenesis on IscSMtb, choosing polar and surface-exposed amino acids in the interaction-sensitive IscSMtb regions. As shown in Supplementary Figure S6(A) (http://www.biochemj.org/bj/459/bj4590467add.htm), several single, double and triple point mutations were generated and tested for complementation in the slow-growing Δ*iscS*Mtb strain. Both tryptophan residue mutations led to only partial complementation. Alanine exchange of the first two arginine residues in the motif had no effect on complementation, whereas triple mutations of Arg^{90}–Arg^{92} led to complete abrogation of IscS complementation on the Δ*iscS* background. However, when expression levels of these mutated proteins were quantified by LC–MS/MS, significantly smaller amounts of protein could be detected compared with the wild-type protein, indicating that the mutated amino acids are essential for protein stability (Supplementary Figure S6B). To rule out promoter mutations in the mycobacterial expression plasmid that might explain the low levels of expressed protein, we individually cloned the mutated IscSMtb genes into an *E. coli* expression vector and purified the proteins from *E. coli* lysates. The resulting expression levels of the mutated proteins were equally low in comparison with the wild-type protein (results not shown). Again, this indicates that the affected amino acids are important for structural integrity of IscSMtb making it difficult to draw conclusions on their individual role in protein–protein interactions.

DISCUSSION

In the present study we generated genetic, structural and functional data to characterize the role of the mycobacterial cysteine desulfurase IscS in Fe–S cluster biogenesis. The largely depleted and unusual ISC operon found in mycobacteria and other Gram-positive bacteria initially led to the assumption that these organisms rely exclusively on the SUF system for Fe–S cluster assembly and repair [13,39]. However, we provide evidence that the deletion of *iscS* in *M. tuberculosis* leads to a phenotype which is associated with dysfunctional Fe–S cluster assembly. Since the typical scaffold proteins for cluster assembly and transfer are absent from the actinobacterial ISC operon, two scenarios for IscSMtb-mediated Fe–S cluster assembly are conceivable: (i) IscSMtb makes use of so far unidentified mycobacterial scaffold proteins or scaffold proteins of the SUF system; or (ii) a direct interaction of IscSMtb and apo-acceptor proteins is involved in sulfur transfer mediated by IscSMtb.

The latter theory of scaffold-protein-independent cluster assembly is supported by data on the mutational analysis of the ISC operon of Gram-negative bacteria. The complementation of an *E. coli* strain lacking the complete ISC operon with IscSEc alone partially restored the activity of some Fe–S-dependent enzymes, clearly indicating that IscS is capable of contributing

to Fe–S cluster formation even in the absence of the scaffold protein IscU [40]. It is well known that IscS has a general Fe–S cluster biogenesis-independent role in sulfur trafficking. A downstream gene product of both the *C. difficile* ISC operon and the *M. tuberculosis* ISC operon is the 2-thiouridylase TrmU (Figure 1), a non-Fe–S enzyme that has been shown to receive sulfur from IscS for the formation of 2-thiouridine in *E. coli* tRNA [41]. Another example of sulfur donation by IscS is thiamine biosynthesis involving the non-Fe–S protein ThiI [42]. These data clearly indicate that IscS can be a direct sulfur donor to several effector proteins. It is thus conceivable that IscS provides sulfur not only to non-Fe–S proteins by direct protein interaction, but also to the apo-forms of Fe–S proteins. Our protein–protein interaction studies, together with the data on impaired Acn and SdhB activity in the mutant strain, support this theory which represents a novel and so far undescribed mechanism of direct sulfur transfer to Fe–S proteins.

This raises the question of why *M. tuberculosis* performs IscU-independent cluster assembly. It was recently shown that the ISC-system in *E. coli* is inactivated by ROS, whereas the SUF system is induced and active only under oxidizing stress mediated by ROS [43]. The labile element within the ISC operon was identified as IscU. Clusters built on this protein were easily oxidized and destroyed, whereas IscS itself retained full activity when exposed to ROS [3,43]. Intracellular mycobacteria encounter a hostile environment in which macrophages constantly produce ROS and reactive nitrogen species that have potent antimicrobial activity. *M. tuberculosis* has evolved several strategies to withstand this stress and to persist within human phagocytes [44]. A ROS-labile IscU protein may be unfavourable for survival in this intracellular niche, and IscS-driven cluster assembly independent of IscU could be a requisite to promote intracellular survival. Our data showing that high levels of IscS protect from H_2O_2 killing support this theory.

We were surprised by our finding that IscSMtb converted L-selenocysteine into L-alanine in a highly efficient and specific way. In fact, the activity of the enzyme was higher in the presence of L-selenocysteine than in the presence of L-cysteine. The *M. tuberculosis* genome lacks genes involved in the biogenesis of selenoproteins including selenocysteine-specific tRNAs and selenophosphate synthase, which was shown to be an acceptor of IscS-derived selenium in other organisms [45]. However, in the presence of selenium, bacteria synthesize L-selenocysteine through the cysteine biosynthesis pathway leading to its unspecific misincorporation into proteins [46]. This effect is even more pronounced in bacteria lacking specific selenium-incorporation pathways, as is the case for *M. tuberculosis* [46]. Owing to the high reduction potential, free L-selenocysteine is considered toxic to the cell, thus IscSMtb could be involved in the detoxification of this highly reactive amino acid.

Another unsolved problem in mycobacterial Fe–S assembly is the source of iron. In *E. coli*, there is some evidence that the bacterial frataxin CyaY may function as an iron donor or at least as an iron-sensing protein during Fe–S cluster assembly on IscU. In addition, there are *in vitro* data implying that IscA may provide iron for the *E. coli* ISC system [2]. However, no CyaY or IscA homologue can be identified in the mycobacterial genome. Further studies are needed to answer these important questions.

In the present study, we have addressed the strong genomic variability of ISC operons found in different organisms. This variability implies distinct Fe–S cluster-assembly mechanisms and structural differences of the respective ISC proteins. In fact, the IscSMtb structure we solved mirrors adaptations made in response to an operon devoid of scaffold proteins since the protein lacks a C-terminal helix that is involved in the formation of the IscS–IscU complex in *E. coli* [35]. Interestingly, it was shown previously that *E. coli* IscU binds to an IscS region rich in amino acids with negatively charged residues [34]. Consistent with charge-dependent protein–protein interactions, it is the IscU mutation K103E (positive to negative) that abrogates the IscS–IscU interaction. We were able to show in the present study that the surface of IscSMtb predominantly contains negatively charged residues and the electrostatic potential, especially in the vicinity of the active site, is highly divergent in IscSMtb and IscSEc. This overall negative net charge in IscSMtb may be a requirement for sulfur transfer to Fe–S proteins, which often carry positively charged Fe–S active sites [47,48].

In conclusion, the results of the present study provide insight into a novel mechanism by which *M. tuberculosis* copes with environmental stress through Fe–S cluster biogenesis and/or repair by the versatile enzyme IscS. It is evident that IscS plays a decisive role in sulfur trafficking and sulfur metabolic pathways which are essential for survival and virulence of *M. tuberculosis* [49]. Its unique structural features not present in IscS proteins of many other bacteria or the human IscS-like protein may provide opportunities for therapeutic interventions against this important pathogen.

AUTHOR CONTRIBUTION

Jan Rybniker envisaged the project. Jan Rybniker, Jeffrey Chen and Gaëlle Kolly performed the gene knockouts. Jan Rybniker, Pia Hartmann and Edeltraud van Gumpel performed Y2H assays. Jan Marienhagen performed the IscS enzymatic assays. Jan Rybniker performed enzymatic assays with *M. tuberculosis* whole-cell lysates. Jan Rybniker and Florence Pojer established the protocols in protein purification and crystallization and determined the crystal structures of IscS. All authors contributed to the development of the paper.

ACKNOWLEDGEMENTS

We thank Diego Chiappe, Romain Hamelin and Dr Marc Moniatte (Proteomics Core Facility, EPFL, Lausanne, Switzerland) for mass spectrometric analysis of IscS protein samples and Professor Matteo dal Peraro, Matteo Thomas Degiacomi and Veronica Monticone (Laboratory for Biomolecular Modeling, EPFL, Lausanne, Switzerland) for their help with the electrostatic surface potential maps.

FUNDING

This work was supported by the BMBF (Bundesministerium für Bildung und Forschung) [grant number 01KI1017 to (J.R. and P.H.)] and the Swiss National Science Foundation [grant number 31003A_140778]. J.M.C. is a recipient of postdoctoral fellowships from the Canadian Thoracic Society and Canadian Institutes of Health Research.

REFERENCES

1 Johnson, D. C., Dean, D. R., Smith, A. D. and Johnson, M. K. (2005) Structure, function, and formation of biological iron–sulfur clusters. Annu. Rev. Biochem. **74**, 247–281
2 Py, B. and Barras, F. (2010) Building Fe–S proteins: bacterial strategies. Nat. Rev. Microbiol. **8**, 436–446
3 Py, B., Moreau, P. L. and Barras, F. (2011) Fe–S clusters, fragile sentinels of the cell. Curr. Opin. Microbiol. **14**, 218–223
4 Bandyopadhyay, S., Chandramouli, K. and Johnson, M. K. (2008) Iron–sulfur cluster biosynthesis. Biochem. Soc. Trans. **36**, 1112–1119
5 Takahashi, Y. and Tokumoto, U. (2002) A third bacterial system for the assembly of iron–sulfur clusters with homologs in archaea and plastids. J. Biol. Chem. **277**, 28380–28383
6 Takahashi, Y. and Nakamura, M. (1999) Functional assignment of the ORF2-iscS-iscU-iscA-hscB-hscA-fdx-ORF3 gene cluster involved in the assembly of Fe–S clusters in *Escherichia coli*. J. Biochem. **126**, 917–926
7 Hidese, R., Mihara, H. and Esaki, N. (2011) Bacterial cysteine desulfurases: versatile key players in biosynthetic pathways of sulfur-containing biofactors. Appl. Microbiol. Biotechnol. **91**, 47–61
8 Schwartz, C. J., Djaman, O., Imlay, J. A. and Kiley, P. J. (2000) The cysteine desulfurase, IscS, has a major role in *in vivo* Fe–S cluster formation in *Escherichia coli*. Proc. Natl. Acad. Sci. U.S.A. **97**, 9009–9014

9 Tokumoto, U., Kitamura, S., Fukuyama, K. and Takahashi, Y. (2004) Interchangeability and distinct properties of bacterial Fe–S cluster assembly systems: functional replacement of the isc and suf operons in *Escherichia coli* with the nifSU-like operon from *Helicobacter pylori*. J. Biochem. **136**, 199–209

10 Muhlenhoff, U., Balk, J., Richhardt, N., Kaiser, J. T., Sipos, K., Kispal, G. and Lill, R. (2004) Functional characterization of the eukaryotic cysteine desulfurase Nfs1p from *Saccharomyces cerevisiae*. J. Biol. Chem. **279**, 36906–36915

11 Kispal, G., Csere, P., Prohl, C. and Lill, R. (1999) The mitochondrial proteins Atm1p and Nfs1p are essential for biogenesis of cytosolic Fe/S proteins. EMBO J. **18**, 3981–3989

12 Tantalean, J. C., Araya, M. A., Saavedra, C. P., Fuentes, D. E., Perez, J. M., Calderon, I. L., Youderian, P. and Vasquez, C. C. (2003) The *Geobacillus stearothermophilus* V *iscS* gene, encoding cysteine desulfurase, confers resistance to potassium tellurite in *Escherichia coli* K-12. J. Bacteriol. **185**, 5831–5837

13 Huet, G., Daffe, M. and Saves, I. (2005) Identification of the Mycobacterium tuberculosis SUF machinery as the exclusive mycobacterial system of [Fe–S] cluster assembly: evidence for its implication in the pathogen's survival. J. Bacteriol. **187**, 6137–6146

14 Mihara, H. and Esaki, N. (2002) Bacterial cysteine desulfurases: their function and mechanisms. Appl. Microbiol. Biotechnol. **60**, 12–23

15 Singh, A., Crossman, D. K., Mai, D., Guidry, L., Voskuil, M. I., Renfrow, M. B. and Steyn, A. J. (2009) *Mycobacterium tuberculosis* WhiB3 maintains redox homeostasis by regulating virulence lipid anabolism to modulate macrophage response. PLoS Pathog. **5**, e1000545

16 Singh, A., Guidry, L., Narasimhulu, K. V., Mai, D., Trombley, J., Redding, K. E., Giles, G. I., Lancaster, Jr, J. R. and Steyn, A. J. (2007) *Mycobacterium tuberculosis* WhiB3 responds to O_2 and nitric oxide via its [4Fe–4S] cluster and is essential for nutrient starvation survival. Proc. Natl. Acad. Sci. U.S.A. **104**, 11562–11567

17 Rybniker, J., Nowag, A., van Gumpel, E., Nissen, N., Robinson, N., Plum, G. and Hartmann, P. (2010) Insights into the function of the WhiB-like protein of mycobacteriophage TM4: a transcriptional inhibitor of WhiB2. Mol. Microbiol. **77**, 642–657

18 Alam, M. S., Garg, S. K. and Agrawal, P. (2009) Studies on structural and functional divergence among seven WhiB proteins of *Mycobacterium tuberculosis* H37Rv. FEBS J. **276**, 76–93

19 Davis, N. K. and Chater, K. F. (1992) The *Streptomyces coelicolor* whiB gene encodes a small transcription factor-like protein dispensable for growth but essential for sporulation. Mol. Gen. Genet. **232**, 351–358

20 Soliveri, J. A., Gomez, J., Bishai, W. R. and Chater, K. F. (2000) Multiple paralogous genes related to the *Streptomyces coelicolor* developmental regulatory gene whiB are present in *Streptomyces* and other actinomycetes. Microbiology **146**, 333–343

21 Saini, V., Farhana, A., Glasgow, J. N. and Steyn, A. J. (2012) Iron–sulfur cluster proteins and microbial regulation: implications for understanding tuberculosis. Curr. Opin. Chem. Biol. **16**, 45–53

22 Munujos, P., Coll-Canti, J., Gonzalez-Sastre, F. and Gella, F. J. (1993) Assay of succinate dehydrogenase activity by a colorimetric-continuous method using iodonitrotetrazolium chloride as electron acceptor. Anal. Biochem. **212**, 506–509

23 Kabsch, W. (2010) Xds. Acta Crystallogr. D Biol. Crystallogr. **66**, 125–132

24 McCoy, A. J., Grosse-Kunstleve, R. W., Adams, P. D., Winn, M. D., Storoni, L. C. and Read, R. J. (2007) Phaser crystallographic software. J. App. Crystallogr. **40**, 658–674

25 Winn, M. D., Ballard, C. C., Cowtan, K. D., Dodson, E. J., Emsley, P., Evans, P. R., Keegan, R. M., Krissinel, E. B., Leslie, A. G., McCoy, A. et al. (2011) Overview of the CCP4 suite and current developments. Acta Crystallogr. D Biol. Crystallogr. **67**, 235–242

26 Murshudov, G. N., Vagin, A. A. and Dodson, E. J. (1997) Refinement of macromolecular structures by the maximum-likelihood method. Acta Crystallogr. D Biol. Crystallogr. **53**, 240–255

27 Sassetti, C. M., Boyd, D. H. and Rubin, E. J. (2003) Genes required for mycobacterial growth defined by high density mutagenesis. Mol. Microbiol. **48**, 77–84

28 Castro-Garza, J., Barrios-Garcia, H. B., Cruz-Vega, D. E., Said-Fernandez, S., Carranza-Rosales, P., Molina-Torres, C. A. and Vera-Cabrera, L. (2007) Use of a colorimetric assay to measure differences in cytotoxicity of *Mycobacterium tuberculosis* strains. J. Med. Microbiol. **56**, 733–737

29 Hsu, T., Hingley-Wilson, S. M., Chen, B., Chen, M., Dai, A. Z., Morin, P. M., Marks, C. B., Padiyar, J., Goulding, C., Gingery, M. et al. (2003) The primary mechanism of attenuation of bacillus Calmette–Guerin is a loss of secreted lytic function required for invasion of lung interstitial tissue. Proc. Natl. Acad. Sci. U.S.A. **100**, 12420–12425

30 Nakayashiki, T., Saito, N., Takeuchi, R., Kadokura, H., Nakahigashi, K., Wanner, B. L. and Mori, H. (2013) The tRNA thiolation pathway modulates the intracellular redox state in *Escherichia coli*. J. Bacteriol. **195**, 2039–2049

31 Mihara, H., Kurihara, T., Yoshimura, T. and Esaki, N. (2000) Kinetic and mutational studies of three NifS homologs from *Escherichia coli*: mechanistic difference between L-cysteine desulfurase and L-selenocysteine lyase reactions. J. Biochem. **127**, 559–567

32 Mihara, H., Kato, S., Lacourciere, G. M., Stadtman, T. C., Kennedy, R. A., Kurihara, T., Tokumoto, U., Takahashi, Y. and Esaki, N. (2002) The *iscS* gene is essential for the biosynthesis of 2-selenouridine in tRNA and the selenocysteine-containing formate dehydrogenase H. Proc. Natl. Acad. Sci. U.S.A. **99**, 6679–6683

33 Tokumoto, U., Nomura, S., Minami, Y., Mihara, H., Kato, S., Kurihara, T., Esaki, N., Kanazawa, H., Matsubara, H. and Takahashi, Y. (2002) Network of protein–protein interactions among iron–sulfur cluster assembly proteins in *Escherichia coli*. J. Biochem. **131**, 713–719

34 Shi, R., Proteau, A., Villarroya, M., Moukadiri, I., Zhang, L., Trempe, J. F., Matte, A., Armengod, M. E. and Cygler, M. (2010) Structural basis for Fe–S cluster assembly and tRNA thiolation mediated by IscS protein–protein interactions. PLoS Biol. **8**, e1000354

35 Urbina, H. D., Silberg, J. J., Hoff, K. G. and Vickery, L. E. (2001) Transfer of sulfur from IscS to IscU during Fe/S cluster assembly. J. Biol. Chem. **276**, 44521–44526

36 Cupp-Vickery, J. R., Urbina, H. and Vickery, L. E. (2003) Crystal structure of IscS, a cysteine desulfurase from *Escherichia coli*. J. Mol. Biol. **330**, 1049–1059

37 Pettersen, E. F., Goddard, T. D., Huang, C. C., Couch, G. S., Greenblatt, D. M., Meng, E. C. and Ferrin, T. E. (2004) UCSF Chimera: a visualization system for exploratory research and analysis. J. Comput. Chem. **25**, 1605–1612

38 Prischi, F., Konarev, P. V., Iannuzzi, C., Pastore, C., Adinolfi, S., Martin, S. R., Svergun, D. I. and Pastore, A. (2010) Structural bases for the interaction of frataxin with the central components of iron–sulphur cluster assembly. Nat. Commun. **1**, 95

39 Albrecht, A. G., Peuckert, F., Landmann, H., Miethke, M., Seubert, A. and Marahiel, M. A. (2011) Mechanistic characterization of sulfur transfer from cysteine desulfurase SufS to the iron-sulfur scaffold SufU in *Bacillus subtilis*. FEBS Lett. **585**, 465–470

40 Tokumoto, U. and Takahashi, Y. (2001) Genetic analysis of the isc operon in *Escherichia coli* involved in the biogenesis of cellular iron–sulfur proteins. J. Biochem. **130**, 63–71

41 Kambampati, R. and Lauhon, C. T. (2003) MnmA and IscS are required for *in vitro* 2-thiouridine biosynthesis in *Escherichia coli*. Biochemistry **42**, 1109–1117

42 Kambampati, R. and Lauhon, C. T. (2000) Evidence for the transfer of sulfane sulfur from IscS to ThiI during the *in vitro* biosynthesis of 4-thiouridine in *Escherichia coli* tRNA. J. Biol. Chem. **275**, 10727–10730

43 Jang, S. and Imlay, J. A. (2010) Hydrogen peroxide inactivates the *Escherichia coli* Isc iron–sulphur assembly system, and OxyR induces the Suf system to compensate. Mol. Microbiol. **78**, 1448–1467

44 Piddington, D. L., Fang, F. C., Laessig, T., Cooper, A. M., Orme, I. M. and Buchmeier, N. A. (2001) Cu,Zn superoxide dismutase of *Mycobacterium tuberculosis* contributes to survival in activated macrophages that are generating an oxidative burst. Infect. Immun. **69**, 4980–4987

45 Cole, S. T., Brosch, R., Parkhill, J., Garnier, T., Churcher, C., Harris, D., Gordon, S. V., Eiglmeier, K., Gas, S., Barry, III, C. E. et al. (1998) Deciphering the biology of *Mycobacterium tuberculosis* from the complete genome sequence. Nature **393**, 537–544

46 Muller, S., Heider, J. and Bock, A. (1997) The path of unspecific incorporation of selenium in *Escherichia coli*. Arch. Microbiol. **168**, 421–427

47 Beinert, H., Kennedy, M. C. and Stout, C. D. (1996) Aconitase as iron–sulfur protein, enzyme, and iron-regulatory protein. Chem. Rev. **96**, 2335–2374

48 Nicolet, Y., Rubach, J. K., Posewitz, M. C., Amara, P., Mathevon, C., Atta, M., Fontecave, M. and Fontecilla-Camps, J. C. (2008) X-ray structure of the [FeFe]-hydrogenase maturase HydE from *Thermotoga maritima*. J. Biol. Chem. **283**, 18861–18872

49 Hatzios, S. K. and Bertozzi, C. R. (2011) The regulation of sulfur metabolism in *Mycobacterium tuberculosis*. PLoS Pathog. **7**, e1002036

Received 25 June 2013/20 January 2014; accepted 19 February 2014
Published as BJ Immediate Publication 19 February 2014, doi:10.1042/BJ20130732

Biochem. J. (2014) **459**, 467–478 (Printed in Great Britain) doi:10.1042/BJ20130732

online data

SUPPLEMENTARY ONLINE DATA

The cysteine desulfurase IscS of *Mycobacterium tuberculosis* is involved in iron–sulfur cluster biogenesis and oxidative stress defence

Jan RYBNIKER*†[1], Florence POJER*, Jan MARIENHAGEN‡, Gaëlle S. KOLLY*, Jeffrey M. CHEN*, Edeltraud VAN GUMPEL†, Pia HARTMANN†§ and Stewart T. COLE*

*Global Health Institute, Ecole Polytechnique Fédérale de Lausanne (EPFL), CH-1015 Lausanne, Switzerland
†1st Department of Internal Medicine, University of Cologne, D-50937 Cologne, Germany
‡Institut für Bio- und Geowissenschaften, IBG-1: Biotechnologie, Forschungszentrum Jülich GmbH, D-52425 Jülich, Germany
§Institute for Medical Microbiology, Immunology and Hygiene, University of Cologne, D-50937 Cologne, Germany

MATERIALS AND METHODS

LC–MS/MS

Gel pieces containing protein of the appropriate molecular mass were first reduced and alkylated (DTE/iodoacetamide). Proteolytic digestion was performed overnight at 37 °C using trypsin in 50 mM ammonium bicarbonate (pH 8.3). Peptides were then extracted from gels and concentrated by SpeedVac before LC–MS/MS measurements. Dried samples were resuspended in LC–MS/MS loading solvent (2 % acetonitrile and 0.1 % formic acid) and separated by HPLC (Ultimate 3000; Dionex). Samples were first captured on a capillary pre-column (Magic C_{18}; 3 μm; 200 Å; 2 cm$\times$100 μm) before analytical separation. An 80 min biphasic gradient was run, starting from 100 % solvent A (2 % acetonitrile and 0.1 % formic acid) to 90 % solvent B (90 % acetonitrile and 0.1 % formic acid) on a capillary column (Nikkyo Technos; C_{18}; 3 μm; 100 Å; 15 cm$\times$75 μm internal diameter; 250 nl/min). Online MS detection was performed on an Orbitrap Elite mass spectrometer (Thermo Scientific) using the data-dependent acquisition mode with dynamic exclusion. For each MS scan, the 20 most intense detected ions were fragmented and then excluded for the following 30 s.

Experimentally generated data were submitted to protein database search through Proteome Discoverer 1.3 and Mascot 2.3 search engine using the UniProt (version Swissprot_2012_03) or TubercuList (Release 25) database. Scaffold 3 Viewer was used to finally compile data results.

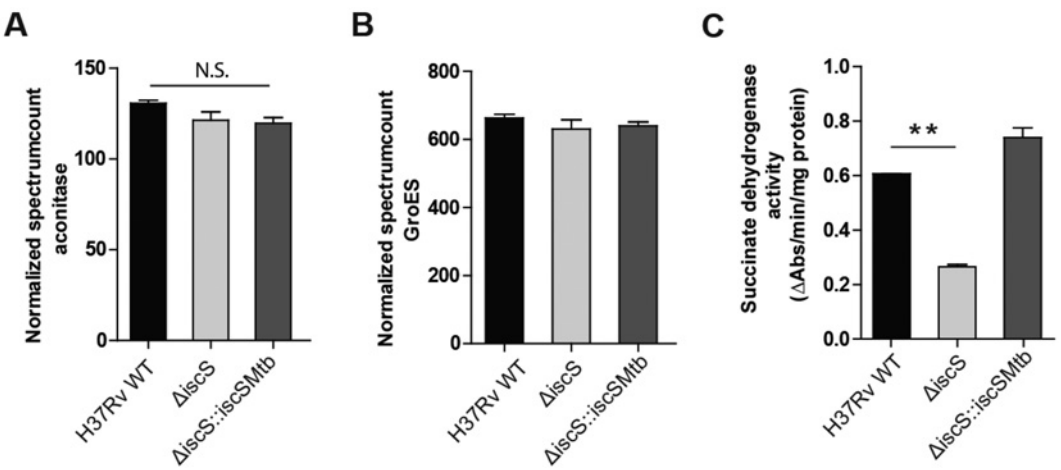

Figure S1 LC–MS/MS quantification

(**A**) LC–MS/MS quantification of Acn from *M. tuberculosis* whole-cell lysates. (**B**) The heat-shock protein GroES was quantified in the same samples and used as a loading control. (**C**) SdhB activity of whole-cell lysates; the Δ*iscS* mutant shows significantly less activity than wild-type and complemented mutant. Results are means ± S.E.M. $^{**}P < 0.01$. N.S.: not significant.

[1] To whom correspondence should be addressed (email jan.rybniker@epfl.ch).
Co-ordinates and structure factors for *Mycobacterium tuberculosis* IscS have been deposited in the PDB under accession code 4ISY.

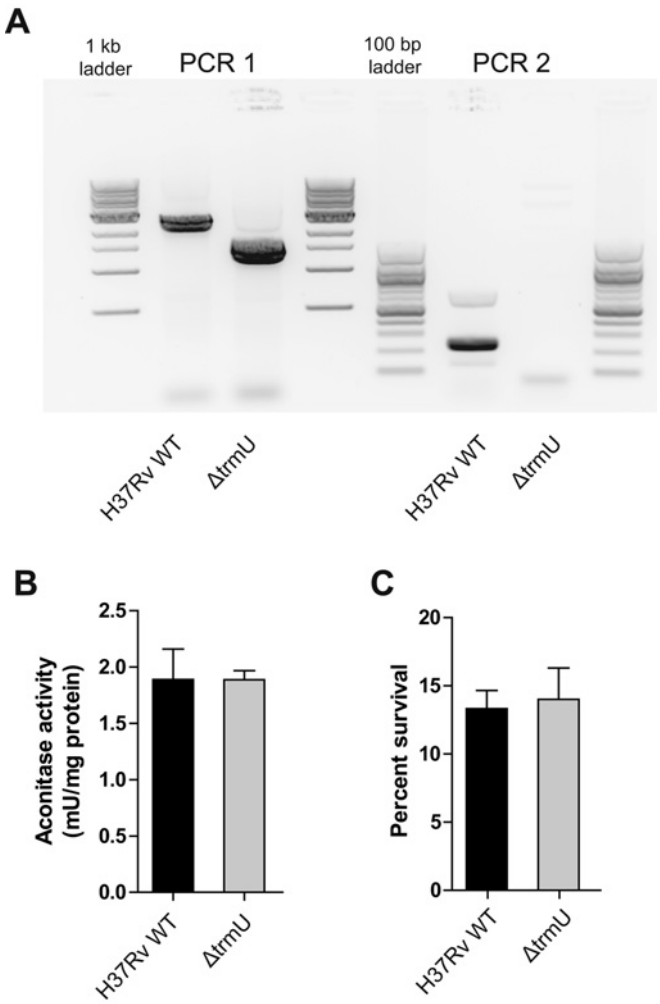

Figure S2 Unmarked deletion of *trmU* in *M. tuberculosis*

(**A**) PCRs to confirm successful deletion. PCR1 spans *trmU* and parts of the flanking genes. PCR2 targets *trmU*. Acn activity (**B**) and H_2O_2 sensitivity (**C**) of the Δ*trmU* mutant and wild-type *M. tuberculosis*. Results are means ± S.E.M. WT, wild-type.

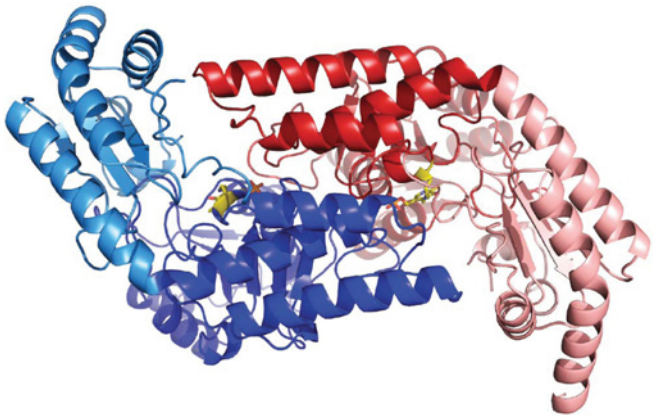

Figure S3 Overall structure of the IscSMtb dimer

The monomers of the dimer are shown in red and blue. Like many PLP-dependent enzymes, each IscSMtb monomer consists of a small and a large domain. Small domains cover amino acids 1–12 and 261–386, which are shown in light blue and light red. The PLP-binding Lys^{205} and the PLP cofactor are labelled in yellow.

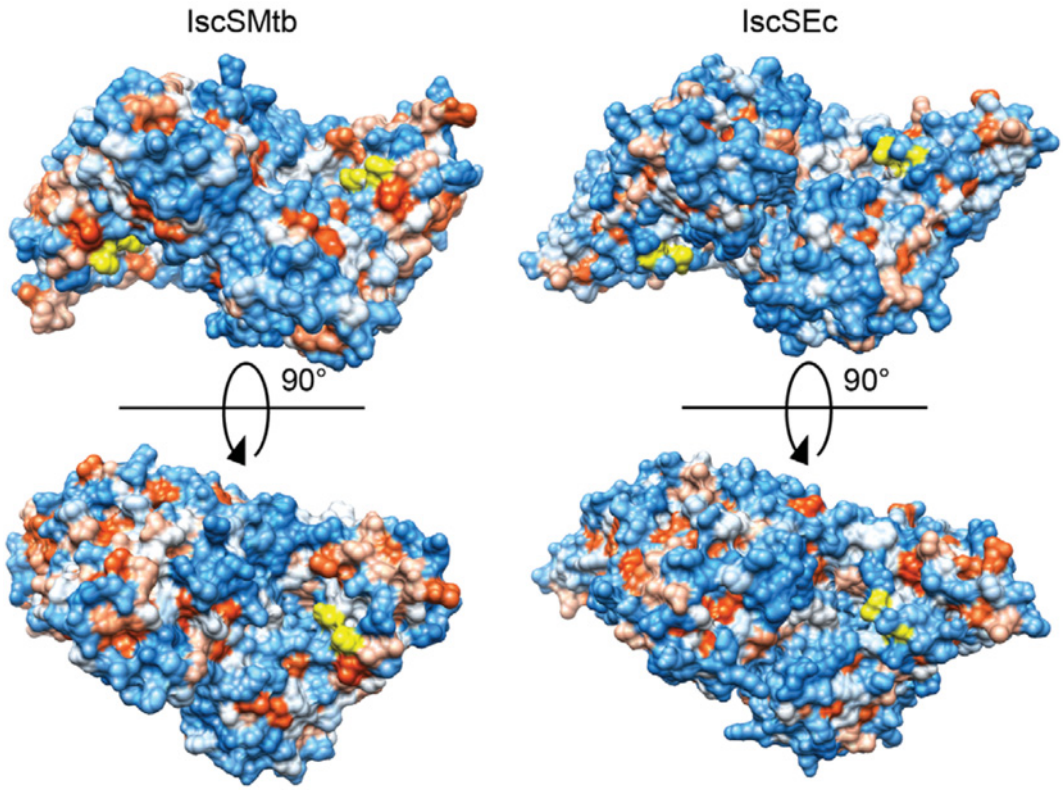

Figure S4 Surface hydrophobicity representation of IscSMtb and IscSEc structures (PDB codes 4ISY and 1P3W)

Blue areas represent hydrophilic amino acids, whereas orange represents areas that are more hydrophobic. The approximate position of the active-site loop, which does not show electron density in both models, is displayed by yellow labelling of the loop flanking the N- and C-terminal amino acids.

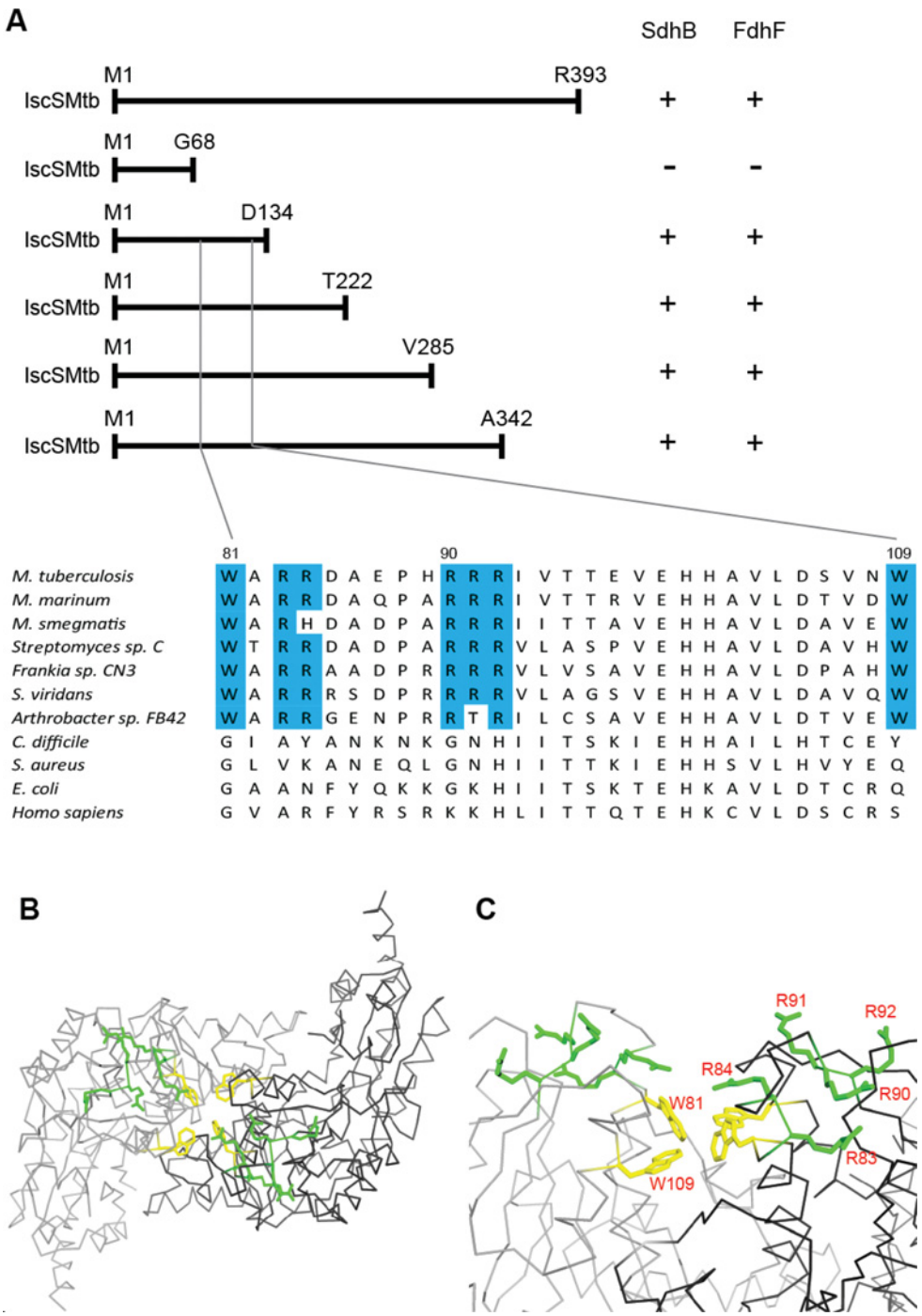

Figure S5 Deletion mapping of domains essential for IscS–protein interaction

(**A**) Upper panel: stepwise deletion of the N-terminal part of the protein was performed and the shortened genes were probed in Y2H assays with two mycobacterial Fe–S proteins (SdhB and FdhF). The N-terminal part up to Asp^{134} is essential for protein interaction. The sequence between Gly^{68} and Asp^{134} was aligned with the respective sequence of IscSEc. Lower panel: alignment of IscS sequences of different bacterial species and the human IscS homologue. *M. marinum*, *Mycobacterium marinum*; *M. smegmatis*, *Mycobacterium smegmatis*; *S. viridans*, *Streptococcus viridans*; *S. aureus*, *Staphylococcus aureus*. The $WXRRX_5RRRX_{16}W$ motif, that is highly conserved in actinomycetes which harbour a reduced ISC operon devoid of scaffold proteins, is indicated in blue. His^{100} is part of the active-site pocket and conserved in all species. (**B**) Top view of the IscSMtb dimer (monomers in light and dark grey) with highlighted $WXRRX_5RRRX_{16}W$ motif. Arginine residues are green and tryptophan residues are yellow. (**C**) Magnified and side view of the same region. Colour coding as in (**B**).

A

Mutation	Complementation
Wild-type	+
C329A (active site cysteine)	-
W81A	+/-
W109A	+/-
W81A/W109A	-
R83-84A	+
R92A	+
R90-92A	-

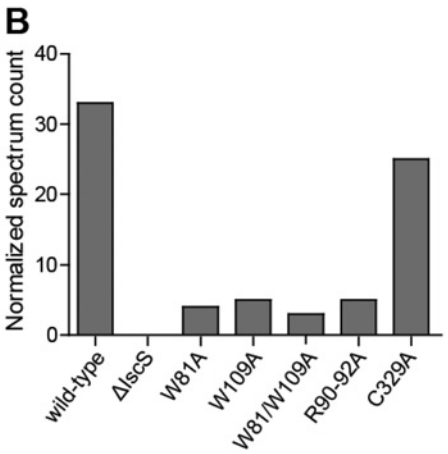

Figure S6 Mutations performed on IscSMtb by alanine scanning and the phenotype of Δ*iscS* strains overexpressing these mutated proteins with regard to growth rate

(**A**) Alanine exchange of the active-site Cys^{329} abrogates IscS activity and the growth rate of this strain (C329A) is as slow as that of the non-complemented Δ*iscS* strain. Similar results were obtained for the W81A, W109A and the R90-92A mutants. (**B**) When the expression levels of these mutated proteins were quantified by LC–MS/MS, only IscSMtb C329A showed levels comparable with the wild-type protein. Representative data from three individual experiments are shown.

Table S1 Plasmids used in the present study

HSP60, heat-shock protein 60.

Plasmid	Description	Source/reference
pQE80L	Expression vector carrying the *cis-laqIq* repressor gene	Qiagen
pQE80:*iscS*Mtb	Expression of His_6-tagged IscSMtb	The present study
pQE80:*iscS*Ec	Expression of His_6-tagged IscSEc	The present study
pETduet-1	Allows expression of S-tagged proteins	Merck
pJG1100	Suicide vector for selection of recombinants and the *sacB* counterselectable marker	[1]
pJG:Rv3026/trmU	pJG1100 carrying the *iscS* flanking genes Rv3026 and *trmU*	The present study
pJG:Rv3023/iscS	pJG1100 carrying the *trmU* flanking genes Rv3023 and *iscS*	The present study
pGA44	Expression plasmid carrying a tetracycline-repressible promoter based on pFRA44 [2]	[3]
pGA44:*iscS*	Plasmid bringing *iscS* under control of the tetracycline-repressible pristinamycin-dependent promoter	The present study
pMV261	Mycobacterial shuttle vector, *HSP60* promoter for protein expression	[4]
pMV261B	pMV261 cut with XbaI and BamHI, PCR product of primers 5 and 6 introduced (see list above): avoids N-terminal fusion of expressed proteins with *HSP60*-derived amino acids	The present study
pMV261B:*iscS*Mtb	Expresses IscSMtb from *HSP60* promoter	The present study
pMV261B:*iscS*Ec	Expresses IscSEc from *HSP60* promoter	The present study
pMD31	Mycobacterial shuttle plasmid	[5]
pMD31:*iscS*Mtb	*iscS* gene with upstream intergenic region for complementation	The present study
pGADT7	Yeast two-hybrid vector	Clontech
pGBKT7	Yeast two-hybrid vector	Clontech
pGADT7:T	Y2H control vector, fusions between the Gal4 activation domain and SV40 large T-antigen	Clontech
pGBKT7:53	Y2H control vector, fusions between the Gal4 DNA-binding domain and murine p53	Clontech
pGADT7:*iscS*Mtb	IscSMtb fusion with Gal4 activation domain	The present study
pGADT7:*iscS*Ec	IscSEc fusion with Gal4 activation domain	The present study
pGADT7:*whiB3*	WhiB3 fusion with Gal4 activation domain	The present study
pGADT7:*sdhB*	SdhB fusion with Gal4 activation domain	The present study
pGADT7:*sirA*	SirA fusion with Gal4 activation domain	The present study
pGADT7:*fdhF*	FdhF fusion with Gal4 activation domain	The present study
pGADT7:*acn*	Acn fusion with Gal4 activation domain	The present study
pGADT7:*trmU*	WhiB3 fusion with Gal4 activation domain	The present study
pGADT7:Rv1456	Rv1465 (mycobacterial IscU homologue) fusion with Gal4 activation domain	The present study
pGBKT7:*whiB3*	WhiB3 fusion with Gal4 DNA-binding domain	The present study
pGBKT7:*sdhB*	SdhB fusion with Gal4 DNA-binding domain	The present study
pGBKT7:*sirA*	SirA fusion with Gal4 DNA-binding domain	The present study
pGBKT7:*fdhF*	FdhF fusion with Gal4 DNA-binding domain	The present study
pGBKT7:*acn*	Acn fusion with Gal4 DNA-binding domain	The present study
pGBKT7:*trmU*	TrmU fusion with Gal4 DNA-binding domain	The present study
pGBKT7:*iscUEc*	IscUEc fusion with Gal4 DNA-binding domain	The present study
pGBKT7:*Rv1465*	Rv1465 (mycobacterial IscU homologue) fusion with Gal4 DNA-binding domain	The present study
pET:*whiB3*	Expression of S-tagged WhiB3	The present study
pET:*acn*	Expression of S-tagged Acn	The present study
pET:*sdhB*	Expression of S-tagged SdhB	The present study

Table S2 Primers used in the present study

qPCR, quantitative PCR.

Primer number	Construct	Primer sequence (5′→3′)
1	pQE80:*iscS*Mtb	TCACCATCACGGATCCGCCTACCTGGATCA
2		TCAGCTAATTAAGCTTTCATCGGGATGCTC
3	pQE80:*iscS*Ec	TCACCATCACGGATCCAAATTACCGATTTATC
4		TCAGCTAATTAAGCTTTTAATGATGAGCCCATTC
5	pMV261B	GATCTTTAAATCTAGAGGTGACCACAACGA
6		TCTGCAGCTGGATCCCATATGTGCGAAGTGATTCCT
7	pMV261B:*iscS*Mtb	TCACTTCGCACATATGGCCTACCTGGATCACGCT
8		AGCTGGATCCCATATGTCATCGGGATGCTCCCG
9	pMV261B:*iscS*Ec	TCACTTCGCACATATGAAATTACCGATTTATC
10		AGCTGGATCCCATATGTTAATGATGAGCCCATTC
11	pMD31:*iscS*Mtb	CGACTCTAGAGGATCCCCGCAGTCACCGAACAC
12		CGGTACCCGGGGATCCTCATCGGGATGCTCCCG
13	pGADT7:*iscS*Mtb	GGAGGCCAGTGAATTCGCCTACCTGGATCA
14		CGAGCTCGATGGATCCTCATCGGGATGCTC
15	pGADT7::*iscS*Ec	GGAGGCCAGTGAATTCAAATTACCGATTTATCTC
16		CGAGCTCGATGGATCCTTAATGATGAGCCCATTC
17	pGBKT7:*whiB3*	GAATTCCCGGGGATCCCACAGCCGGAGCAG
18		GCAGGTCGACGGATCCTTAAGCTGTGCGGC
19	pGBKT7::*sdhB*	GAATTCCCGGGGATCCTGAGCGTCGAGCCGGACGTCGA
20		GCAGGTCGACGGATCCTCAGCGGGTGAACATCAGC
21	pGBKT7:*fdhF*	GAATTCCCGGGGATCCTGTACGTTGAGGCGGTGAGGT
22		GCAGGTCGACGGATCCCTAGGCCGTTGGCTCCAATCGCA
23	pGBKT7:*acn*	GAATTCCCGGGGATCCTGACTAGCAAATCTGTGAA
24		GCAGGTCGACGGATCCTCAGCCTGACTTCAGTATGT
25	pGBKT7:*sirA*	GAATTCCCGGGGATCCTGTCCGCGAAGGAGAAC
26		GCAGGTCGACGGATCCTCATCGCAGGTCGTCCT
27	pGBKT7:*trmU*	GAATTCCCGGGGATCCTGAAAGTTCTCGCC
28		GCAGGTCGACGGATCCTCAAGCCCCGGGGT
29	pGBKT7:*iscUEc*	GAATTCCCGGGGATCCCTTACAGCGAAAAAGTTATC
30		GCAGGTCGACGGATCCTTATTTTGCTTCACGTTTGC
31	pGBKT7:*Rv1465*	GAATTCCCGGGGATCCTGACGTTGCGTCTGGA
32		GCAGGTCGACGGATCCTCAGCCGGTGCGCTGGTT
33	pGADT7:*whiB3*	GGAGGCCAGTGAATTCCCACAGCCGGAGCA
34		CGAGCTCGATGGATCCTTAAGCTGTGCGGC
35	pGADT7:*acn*	GGAGGCCAGTGAATTCACTAGCAAATCTGTGAACT
36		CGAGCTCGATGGATCCTCAGCCTGACTTCAGTATGTT
37	pGADT7:*sdhB*	GGAGGCCAGTGAATTCAGCGTCGAGCCGGACGTCGA
38		CGAGCTCGATGGATCCTCAGCGGGTGAACATCAGC
39	pGADT7:*fdhF*	GGAGGCCAGTGAATTCTACGTTGAGGCGGTGAGGT
40		CGAGCTCGATGGATCCCTAGGCCGTTGGCTCCAAT
41	pGADT7:*sirA*	GGAGGCCAGTGAATTCTCCGCGAAGGAGAACCCCCA
42		CGAGCTCGATGGATCCTCATCGCAGGTCGTCCTCCT
43	pGADT7:*trmU*	GGAGGCCAGTGAATTCAAAGTTCTCGCCGCGATGA
44		CGAGCTCGATGGATCCTCAAGCCCCGGGGTTGCCG
45	pGADT7:Rv1465	GGAGGCCAGTGAATTCACGTTGCGTCTGGAGCAGAT
46		CGAGCTCGATGGATCCTCAGCCGGTGCGCTGGTTTC
47	pGADT7:*iscS*A324	CGAGCTCGATGGATCCTCATGCAATCAACACATGCGAG
48	pGADT7:*iscS*V285	CGAGCTCGATGGATCCTCAAACATCGTCAATCTC
49	pGADT7:*iscS*T222	CGAGCTCGATGGATCCTCAGGTGACGTCGCGGCGCAG
50	pGADT7:*iscS*D134	CGAGCTCGATGGATCCTCAGTCGTCGTGGCTCTGC
51	pGADT7:*iscS*G68	CGAGCTCGATGGATCCTCAGCCGCCCGCGGTGAAG
52	pET:*whiB3*	AAGGAGATATACATATGCCACAGCCGGAGCAGCT
53		CTTTACCAGACTCGAGAGCTGTGCGGCGGATG
54	pET:*acn*	AAGGAGATATACATATGACTAGCAAATCTGTGAA
55		CTTTACCAGACTCGAGGCCTGACTTCAGTATGTT
56	pET:*sdhB*	AAGGAGATATACATATGAGCGTCGAGCCGGACGT
57		TTTACCAGACTCGAGGGTACCGCGGGTGAACATCAGCG
58	pJG:Rv3026/*trmU*	TCGACTCTAGACTTAATTAAATGAGCGCTCCCGCA
59		GAGCATATGCCTAGGCATGACGCACCTAGA
60		TGCGTCATGCCTAGGCGATGAAAGTTCTCG
61		GTACCCGGGGGCGCGCCTCAAGCCCCGGGGTT
62	pJG:Rv3023/*iscS*	GACTCTAGACTTAATTAATCGTCGCTGCACACCAGC
63		CGAGCATATGCCTAGGCATCGGGATGCTCCC
64		CATCCCGATGCCTAGGTGACTCGGCGCCAAATCA
65		GTACCCGGGGGCGCGCCATTCGGCGTCGGGCT
66	pGA44:*iscS*	GCCTGAATGCCTAGGATGGCCTACCTGGAT
67		AAGTTATAACCTAGGTCATCGGGATGCTCC
68	Target, flanking *trmU* genes	GGGCGACATCCCGGTCTCT
69		CGGATCATTGCGTCTCTCGCT
70	Target, *trmU*	CTCGCGGGGCTGTTGTTC

Table S2 Continued

Primer number	Construct	Primer sequence (5′→3′)
71		CGACAGCCGGGCGTAGTG
72	qPCR *iscSMtb*	GACGGACTCGAGGAAAACAG
73		AAAGTGAAGTGCGCGTTACC
74	qPCR *sigA*	TGGACTCATCGATGTTCTTCC
75		TAGGGCTCACCGACCTCTAA
76	Mutagenesis C329A	AACCGGATCGGCCGCCACGGCAGGTGTAG
77		CTACACCTGCCGTGGCGGCCGATCCGGTT
78	Mutagenesis W81A	GGCTGTCAAAGGTATCTATGCCGCACGCCGCG
79		CGCGGCGTGCGGCATAGATACCTTTGACAGCC
80	Mutagenesis W109A	CTGGACTCGGTGAACGCCCTCGTGGAACACGAA
81		TTCGTGTTCCACGAGGGCGTTCACCGAGTCCAG
82	Mutagenesis R83A/R84A	GGTATCTATTGGGCAGCCGCCGATGCGGAGCCGCAC
83		GTGCGGCTCCGCATCGGCGGCTGCCCAATAGATACC
84	Mutagenesis R90A/R91A/R92A	TGCGGAGCCGCACGCCGCAGCCATCGTCACCACCG
85		CGGTGGTGACGATGGCTGCGGCGTGCGGCTCCGCA
86	Mutagenesis R92A	CCGCACCGCCGTGCCATCGTCACCACC
87		GGTGGTGACGATGGCACGGCGGTGCGG

Table S3 Data collection and refinement statistics (molecular replacement)

One crystal for each structure. Values for the highest-resolution shell are shown in parentheses.

Parameter	Value
Data collection	
Space group	P_1
Cell dimensions	
a, *b*, *c* (Å)	66.81, 78.13, 92.77
α, β, γ (°)	94.54, 104.71, 98.57
Resolution (Å)	50–2.59 (2.75–2.59)
R_{meas}	9.3 (31.4)
$I/\sigma I$	11.15 (3.61)
Completeness (%)	94.4 (90.1)
Redundancy	2.50 (2.30)
Refinement	
Resolution (Å)	2.59
Number of reflections	51516
R_{work}/R_{free}	0.19/0.24
Number of atoms	
Protein	11149
Ligand	113
Water	273
B-factor	28.2
RMSD	
Bond lengths (Å)	0.015
Bond angles (°)	1.833

REFERENCES

1 Kirksey, M. A., Tischler, A. D., Simeone, R., Hisert, K. B., Uplekar, S., Guilhot, C. and McKinney, J. D. (2011) Spontaneous phthiocerol dimycocerosate-deficient variants of *Mycobacterium tuberculosis* are susceptible to γ interferon-mediated immunity. Infect. Immun. **79**, 2829–2838

2 Boldrin, F., Casonato, S., Dainese, E., Sala, C., Dhar, N., Palù, G., Riccardi, G., Cole, S. T. and Manganelli, R. (2010) Development of a repressible mycobacterial promoter system based on two transcriptional repressors. Nucleic Acids Res. **38**, e134

3 Kolly, G. S., Boldrin, F., Sala, C., Dhar, N., Hartkoorn, R. C., Ventura, M., Serafini, A., McKinney, J. D., Manganelli, R. and Cole, S. T. (2014) Assessing the essentiality of the decaprenyl-phospho-D-arabinofuranose pathway in *Mycobacterium tuberculosis* using conditional mutants. Mol. Micorbiol., doi:10.1111/mmi.12546

4 Stover, C. K., de la Cruz, V. F., Fuerst, T. R., Burlein, J. E., Benson, L. A., Bennett, L. T., Bansal, G. P., Young, J. F., Lee, M. H. and Hatfull, G. F. (1991) New use of BCG for recombinant vaccines. Nature **351**, 456–460

5 Donnelly-Wu, M. K., Jacobs, Jr, W. R. and Hatfull, G. F. (1993) Superinfection immunity of mycobacteriophage L5: applications for genetic transformation of mycobacteria. Mol. Microbiol. **7**, 407–417

Received 25 June 2013/20 January 2014; accepted 19 February 2014
Published as BJ Immediate Publication 19 February 2014, doi:10.1042/BJ20130732